



Universitat Autònoma de Barcelona

**ADVERTIMENT.** L'accés als continguts d'aquesta tesi queda condicionat a l'acceptació de les condicions d'ús establertes per la següent llicència Creative Commons:  [http://cat.creativecommons.org/?page\\_id=184](http://cat.creativecommons.org/?page_id=184)

**ADVERTENCIA.** El acceso a los contenidos de esta tesis queda condicionado a la aceptación de las condiciones de uso establecidas por la siguiente licencia Creative Commons:  <http://es.creativecommons.org/blog/licencias/>

**WARNING.** The access to the contents of this doctoral thesis it is limited to the acceptance of the use conditions set by the following Creative Commons license:  <https://creativecommons.org/licenses/?lang=en>



**Universitat Autònoma de Barcelona**

**Doctoral program in Medicine**

**Doctoral Thesis**

**AN *IN VIVO* STUDY OF THE IMPORTANCE OF THE INNATE  
IMMUNE SYSTEM IN THE PATHOGENESIS OF EPIDERMOLYSIS  
BULLOSA ACQUISITA**





**Universitat Autònoma de Barcelona**

Programa de doctorat en Medicina. Departament de Medicina

**ESTUDI *IN VIVO* SOBRE LA RELLEVÀNCIA DEL SISTEMA IMMUNE  
INNAT EN LA PATOGÈNIA DE LA EPIDERMÒLISI AMPUL·LAR  
ADQUIRIDA**

Tesi doctoral presentada per:

**Maria Estela Martinez Escala**

Directors:

**Dr. Josep E. Herrero González**

**Dr. Ramon M Pujol Vallverdú**

Barcelona, 2016



*“Once we accept our limits, we go beyond them.”*

*Albert Einstein*



## **ACKNOWLEDGMENT**

---





## **Acknowledgements**

This study has been made possible by the financial support from the Fondo de Investigación Sanitaria, Instituto de Salud Carlos III/FEDER (Spanish Ministry of Science and Innovation) granted to Dr. Josep E. Herrero González (PS09/01410).

The author is greatly indebted with the Molecular Laboratory of Universitätsklinikum Freiburg (Germany) for all of their contributions to this project, including the supply of the protein mCVIICr by Jessica Kleindienst, and the training on the experimental animal model technique by Kinga Melinda Csorba and Florina Florea. I would like to express my sincere gratitude to Dr. Cassian Sitaru for his teaching and guidance throughout the project development.

A specially thank you to Boston Children's Cancer and Blood Disorders Center, which provided us with the Rac2 knock-out mice.

The author also gives thanks to the veterinarians and technicians at the animal facilities of the Parc de Recerca Biomedica de Barcelona, for all their assistance in teaching some of the animal procedures, and to the Department of Pathology of Parc de Salut Mar for the hematoxilin-eosin staining of the murine skin biopsies.

In addition, the author wants to thank the laboratory of Dr. Gabriel Gil, Apoptotic signaling at Parc de Recerca Biomedica de Barcelona, who performed the genotyping of the inbred Rac2 knock-out mice.

The author wants to thank her fellow labmates that helped through the long struggles during the thesis, including Xavier Joya for his assistance in some laboratory techniques, and Dr. Irene Garcia Diez, who assisted me to finish some experiments of this thesis.

The author gives special thanks to Kimberly A. Sable for editing and reviewing the manuscript.

The author wants to give her gratitude to her thesis advisors, Dr. Josep E. Herrero and Dr. Ramon M. Pujol, who both assisted providing their critical opinion and suggestions to improve this work.

Least but not last, the author cannot thank enough to her family and friends for all the support given, not only in this thesis but also in my life project.



## Index

|                                      |           |
|--------------------------------------|-----------|
| <b>1. Abbreviations</b>              | <b>13</b> |
| <b>2. Introduction</b>               | <b>17</b> |
| 2.a. Basement membrane zone          | 19        |
| 2.b. Autoimmune blistering disorders | 22        |
| 2.c. Epidermolysis bullosa acquisita | 24        |
| 2.d. Experimental models of EBA      | 35        |
| <b>3. Background</b>                 | <b>39</b> |
| 3.a. Type VII collagen               | 41        |
| 3.b. Loss of immunological tolerance | 45        |
| 3.c. Tissue injury                   | 46        |
| 3.c.i. Role of complement            | 47        |
| 3.c.ii. Neutrophils                  | 47        |
| 3.c.iii. Fc receptors                | 48        |
| 3.c.iv. Reactive oxygen species      | 49        |
| 3.d. Rac2 protein                    | 53        |
| <b>4. Objectives</b>                 | <b>59</b> |
| <b>5. Materials and methods</b>      | <b>63</b> |
| 5.a. Mice                            | 65        |
| 5.b. Mice genotyping                 | 65        |
| 5.c. Recombinant protein CVII        | 66        |
| 5.d. Rabbit immunization             | 66        |

|   |            |
|---|------------|
| <i>5.e. Affinity purification of IgG</i>      | 67         |
| <i>5.f. Induction of experimental EBA</i>     | 67         |
| <i>5.g. Drug administration</i>               | 68         |
| <i>5.h. Histology</i>                         | 68         |
| <i>5.i. Immunofluorescence microscopy</i>     | 69         |
| <i>5.j. Enzyme linked immunosorbent assay</i> | 69         |
| <i>5.h. Statistical analysis</i>              | 70         |
| <b>6. Results</b>                             | <b>71</b>  |
| <b>7. Discussion</b>                          | <b>99</b>  |
| <b>8. Conclusions</b>                         | <b>107</b> |
| <b>9. References</b>                          | <b>111</b> |

## **1. ABBREVIATIONS**

---

## **1. ABBREVIATIONS**

|         |   |
|---------|---|
| A/J     | Mouse substrain                                   |
| ALI     | Acute lung injuryBALB/C                           |
| BMZ     | Basement membrane zone                            |
| BP      | Bullous pemphigoid                                |
| BPAG1   | Bullous pemphigoid antigen 1                      |
| BPAG2   | Bullous pemphigoid antigen 2                      |
| BSA     | Body surface area                                 |
| C       | Complement (C3, C1q, C5a)                         |
| C57BL/6 | Mouse substrain                                   |
| CaaL    | C-terminal sequence, aliphatic aminoacid, Leucine |
| CCR4    | C-C motif chemokine receptors                     |
| CD      | Cluster of differentiation (CD151, CD4)           |
| CGD     | Chronic granulomatous disease                     |
| CMP     | Cartilage matrix protein                          |
| COL7A1  | Type collagen VII gene                            |
| CVII    | Type VII collagen                                 |
| CXCR    | C-X-C motif chemokine receptors                   |
| CXCL    | C-X-C motif ligand                                |
| DC      | Dendritic cells                                   |
| DEX     | Dexamethasone                                     |
| DIF     | Direct immunofluorescence                         |
| EBA     | Epidermolysis bullosa acquisita                   |
| ELISA   | Enzyme-linked immunesorbent assay                 |
| F(ab)   | Variable portion of antibody                      |

|        |  |
|--------|--|
| Fc     | Fragment crystallizable, constant fragment of the antibody |
| FcR    | Receptor of the constant fragment of antibodies            |
| FITC   | Fluorescein isothiocyanate                                 |
| Fn     | Fibronectin  |
| FOAM   | Fluorescent overlay antigen mapping                        |
| GAP    | GTPases activating protein                                 |
| GDP    | Guanosine diphosphate                                      |
| GDI    | GDP dissociation inhibitors                                |
| GEF    | guanine nucleotide exchange factor                         |
| GM-CSF | Granulocyte-macrophage colony-stimulating factor           |
| Gr-1   | Myeloid differentiation antigen Gr-1                       |
| GTP    | Guanosine triphosphatase                                   |
| GST    | Glutathione-S-transferase                                  |
| HLA    | Human leukocyte antigen                                    |
| Hsp    | Heat shock protein   |
| IBD    | Inflammatory bowel disease                                 |
| IEM    | Immunoelectron microscopy                                  |
| IIF    | Indirect immunofluorescence                                |
| Ig     | Immunoglobulin   |
| IL     | Interleukin  |
| ITAM   | Immunereceptor tyrosine-based activation motif             |
| ITIM   | Immunereceptor tyrosine-based inhibition motif             |
| IV     | Intravenous  |
| KO     | Knock-out  |
| LAD    | Leukocyte adhesion deficiency                              |
| LPS    | lipopolysaccharide   |



|          |   |
|----------|---|
| mCVIIc   | Murine CVII corresponding to fragment Cr    |
| MHC      | Major histocompatibility complex            |
| mg       | milligrams                                  |
| MMP      | Mucous-membrane pemphigoid                  |
| MPO      | Myeloperoxidase                             |
| NADPH    | Nicotinamide adenine dinucleotide phosphate |
| NBT      | Nitroblue-tetrazolium                       |
| NC       | Non-collagen                                |
| NSC23766 | Rac1/Rac2 inhibitor                         |
| Phox     | Phagocytic oxidases                         |
| Rac2     | Ras-related C3 botulinum toxin substrate 2  |
| R-IgG    | Rabbit IgG                                  |
| ROS      | Reactive oxygen species                     |
| SJL-1    | Mouse substrain                             |
| SKH-1    | Mouse substrain                             |
| TEM      | Transmission electron microscopy            |
| vWF      | von Willebrand factor                       |

## **2. INTRODUCTION**

---



## **2. INTRODUCTION**

### *2.a. Basement membrane zone*

The basement membrane zone (BMZ) is a complex structure with different functions including cell adhesion, differentiation, motility, transmission of extracellular signals and growth factors, and formation of permeability barriers (1, 2). Broadly, the main structure is made of intracellular and extracellular proteins, in which some of them are organ-specific (e.g. kidney, lung, skin) proteins, yet others are ubiquitous in all basement membranes of the body, making up the basic scaffolding of the BMZ. Dermal-epidermal BMZ structure is one of the best studied. Structural proteins are interconnected forming different layers from the basal keratinocytes of the epidermis to the dermis, which includes lamina lucida, lamina densa and sublamina densa. Main proteins involved in dermal-epidermal adhesion are represented in figure 1(2). There are two main structures of the dermal-epidermal BMZ that strengthen the attachment among the different layers, the hemidesmosome plaque and the focal adhesions. The hemidesmosome plaque is the main adhesion structure of the dermal-epidermal BMZ that specifically connects the keratin intermediate filaments to lamina lucida. In addition to hemidesmosome plaque, focal adhesions, also known as focal contacts or integrin adhesomes, are located between two different hemidesmosomes and connect actin to the lamina lucida.

The hemidesmosome plaque is formed by plectin, bullous pemphigoid antigen 1 (BPAG1, also known as BP230), integrins ( $\alpha 6\beta 4$ ) and type XVII collagen (also known as BPAG2 or BP180). Integrins and BPAG2 connect to extracellular proteins such as laminins (-332, -311) forming the anchoring filaments. Lamina densa is formed by the interaction of the laminins (-332, -311) plus three additional proteins: nidogen, laminin-511, and type IV collagen. These three additional proteins are found ubiquitously in the BMZ of different organs (non-organ-specific). Finally, structures that extend down from the lamina densa are known as anchoring fibrils and their most abundant component is collagen VII (CVII) (1, 2).

Focal adhesion or integrin adhesomes are formed by integrin  $\alpha3\beta1$  and adhere the actin cytoskeleton to the lamina lucida. It is stated that integrin adhesome has a higher complexity compared with the hemidesmosome structure, which suggests extensive functional diversity. Finally, CD151 is a member of the tetraspan superfamily, also expressed ubiquitously, and is co-distributed with both integrins,  $\alpha3\beta1$  and  $\alpha6\beta4$  (2).

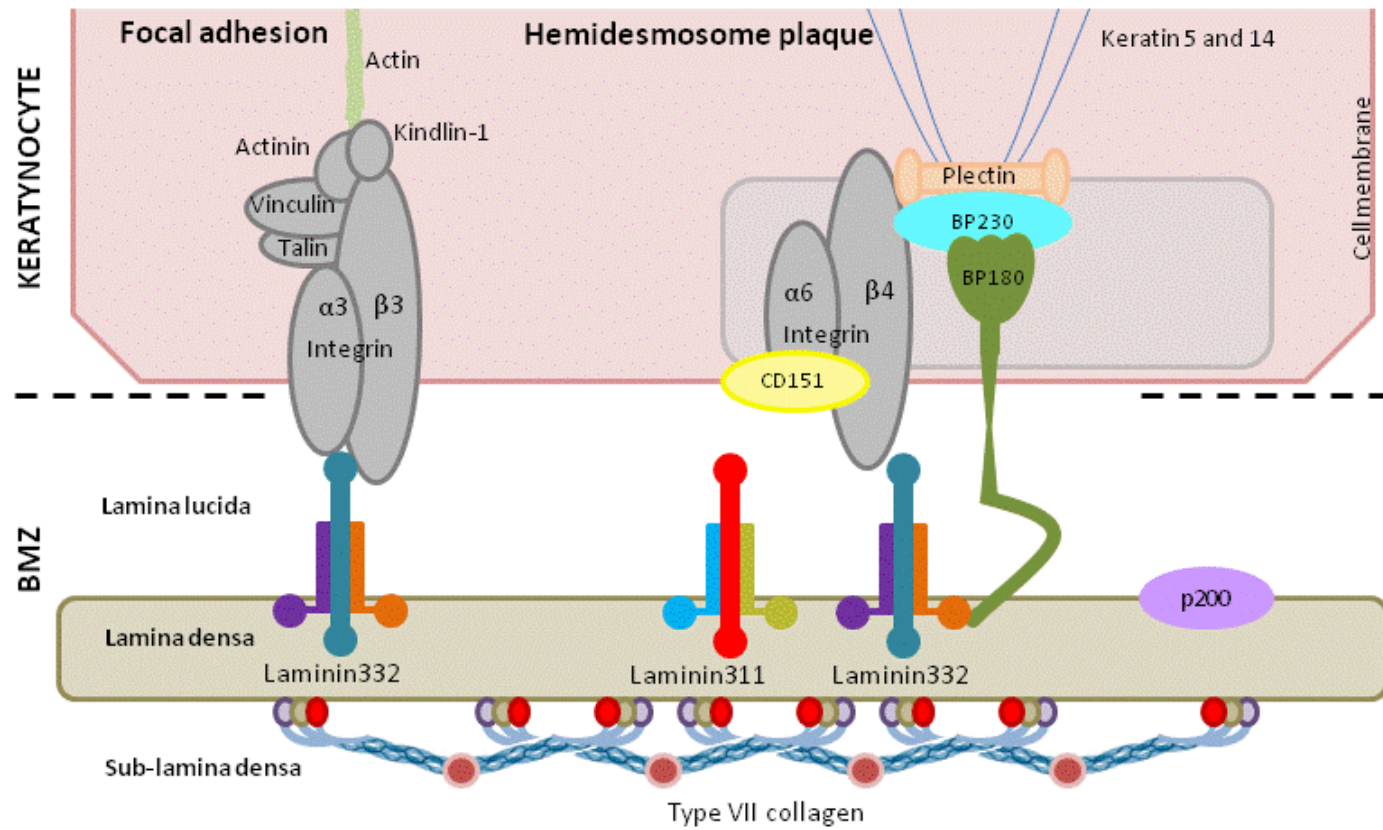


**Figure 1. Dermal-epidermal BMZ.** Structure, main proteins and their distribution forming the BMZ are shown (2).

## *2.b. Autoimmune blistering diseases of the skin*

Autoimmune mucocutaneous blistering diseases are a wide group of rare disorders characterized by the presence of circulating antibodies against different proteins of either cell-to-cell adhesion structures (desmosomes) or BMZ of the skin and mucous membranes. These antibodies induce intraepidermal or dermal-epidermal separation depending on the target protein, which is clinically manifested as blisters, erosions or crusts. The level of blister formation allows classifying these conditions in two distinct groups. First group are the intraepidermal bullous disorders where the proteins involved are desmosomes, plakin family or armadillo family proteins, and they manifest as fragile blisters and erosions. The second group corresponds to the subepidermal bullous disorders, where hemidesmosomes, proteins from the lamina densa and lucida (e.g. laminin and integrins), and anchoring fibrils are the main targets, and typically present with tense blisters. Table 1 shows the different autoimmune bullous diseases with their main associated antigens. This thesis is focused on epidermolysis bullosa acquisita (EBA), which belongs to the second group and where anchoring fibrils are the main target protein of autoantibodies.

**Table 1.** Main target proteins and type of antibodies of each autoimmune bullous disease (3-6).

| Main classification | Disease                              | Protein   | Type of antibody  |
|---------------------|--------------------------------------|---|-------------------|
| Epidermal           | Pemphigus vulgaris                   | Dsg 3 and 1   | IgG               |
|                     | Pemphigus foliaceus                  | Dsg 1   | IgG               |
|                     | Pemphigus vegetans                   | Dsg 3 and 1, Dsc 1 -3   |                   |
|                     | Pemphigus erythematosus              | Dsg 1   |                   |
|                     | Paraneoplastic pemphigus             | Plectin, Epiplakin, Desmoplakin I/II, Envoplakin, Periplakin, A2ML1, Dsg 1, Dsg 3, Dsc 1-3, BP230 | IgG               |
|                     | IgA pemphigus                        | Dsc 1, Dsg 1 and 3  | IgA               |
| Subepidermal        | Bullous pemphigoid                   | BP180, BP230  | IgG/IgE           |
|                     | Pemphigoid gestationis               | BP180 (NC 16a domain)   | IgG               |
|                     | Linear IgA dermatosis                | LAD-1, 97kDa/120kDa   | IgA               |
|                     | Mucous membrane pemphigoid           | BP180, Laminin 332, $\alpha 6$ integrin, $\beta 4$ integrin, 168kDa protein,                      | IgG/IgA           |
|                     | Epidermolysis bullosa acquisita      | CVII  | IgG/IgA           |
|                     | Bullous systemic lupus erythematosus | CVII  | IgG, IgA, C3, C1q |
|                     | Anti-p200 pemphigoid                 | Laminin $\gamma 1$ (subunit of the integrin)  | IgG/IgA           |
|                     | Dermatitis herpetiformis             | Epidermal transglutaminases   | IgA               |

A2ML1: Alpha-2-Macroglobulin Like; Dsg: Desmoglein; Dsc: Desmocollins; NC: Non-collagenous; LAD-1: fragment of the extracellular domain of the BP180, linear IgA dermatosis



### *2.c. Epidermolysis bullosa acquisita*

Epidermolysis bullosa is term defining a group of disorders characterized by the presence of blisters, erosions and crust on the skin and mucous membrane. There are two main groups that can be differentiated, inherited and *acquisita*. The inherited forms are characterized by the deficiency of the specific skin proteins and most of them are present since born. The *acquisita* form is an acquired and chronic autoimmune disease characterized by the presence of circulating autoantibodies against CVII that bind to the BMZ inducing dermal-epidermal separation. It was first described by Elliot and named by Kablitz in 1985, in order to differentiate it from the inherited forms (7-9).

#### *2.c.i. Epidemiology*

EBA is a rare condition with an incidence of 0.2 to 0.5 new cases per million per year (9-11). Even though EBA has been reported in all ages, it commonly presents in adults with a median age of 47 years (75<sup>th</sup> percentile: 30 – 66 years of age). Initially, no predominant gender or ethnic group was noted in EBA patients. However, more recently, three large studies with a total of 83 patients have shown a female to male predominance (61% female versus 39% male) (11-13). Moreover, a genetic association has been established with the major histocompatibility complex (MHC) class II haplotype, in particular human leukocyte antigen (HLA)-DR2. It has been found that EBA is more common among the African American population with DRB1\*15, and in Koreans with DRB1\*13 (14, 15).

#### *2.c.ii. Clinical features*

Tense blisters and erosions in mucocutaneous areas are the main clinical features; however, EBA can present in diverse manners. In broad terms, two clinical forms are differentiated: mechanobullous (or non-inflammatory) and inflammatory (the most

frequent presentation in humans). The first type, also known as the classical form, is seen in only one third of the patients, and usually manifests with blisters, erosions and scars appearing in trauma prone locations, such as fingers and toes, where the loss of nails is characteristic. The inflammatory form is classified in four different subtypes that resemble other types of autoimmune mucocutaneous blistering conditions: bullous pemphigoid (BP)-like EBA, mucous-membrane pemphigoid (MMP)-like EBA, Brunsting-Perry pemphigoid-like EBA and linear IgA dermatitis-like EBA.

BP-like EBA presents with the clinical features of BP or a mixture of BP and the classical form of EBA. Usually lesions are widespread along the trunk and extremities with pruritus. Tense blisters are surrounded by inflamed or urticarial skin, and no scarring or millia formation is seen in contrast to the classical form. In MMP-like EBA, blisters and scars involve the mouth, upper esophagus, conjunctiva, anus and genital mucosa. Involvement of the trachea has been reported, as well as, resolution without scarring of the involved mucosa. Brunsting-Perry pemphigoid-like EBA presents with lesions mainly involving the head and neck and usually leaves residual scars. Mucous membranes are not afflicted in contrast to MMP-like EBA. Linear IgA bullous dermatosis-like EBA presentation is characterized by annular pattern of the tense blisters and mucous membranes are frequently involved.

Although EBA patients are predominantly adults, pediatric cases have also been described with similar clinical manifestations. A study consisting of 14 children showed 5 with IgA linear dermatosis-like EBA, 5 with BP-like EBA, and the remaining 4 presenting as the classical form of EBA (16). Mucosal involvement was observed in 11 of the 14 children, which seemed more severe and frequent when compared to adults. However, the overall prognosis and treatment was more favorable in pediatric than in adult EBA. Mucocutaneous involvement and a higher treatment response were also seen in another study with 33 pediatric patients, which confirmed the data presented previously (11, 12, 17). Finally, congenital EBA has also been described due to the transference of IgG from the mother to the fetus (18).

Overall, the clinical presentation of EBA may change during the course of the disease or may show overlap between the different forms within the same patient. Moreover, the disease will eventually become non-inflammatory over time. Despite of that, disease severity varies from one patient to another and usually correlates with antibody levels. Also, it has been suggested that clinical presentation may correlate with the epitope profile, but this has not yet been fully demonstrated.

With disease progression, these patients develop dramatic consequences, such as dystrophic changes, including atrophic scars that may also involve the scalp, nail deformities and digital contractures (9, 19, 20). Yet mucous membrane involvement can trigger severe sequels. Ocular lesions can be seen in MMP-like EBA patients, which may occasionally progress to complete blindness. Besides the oral and ocular mucous membranes, other areas of great interest due to life-threatening complications are trachea, esophagus and larynx. Esophageal strictures inhibit the passage of food into the stomach and require endoscopic dilation. Lastly, hoarseness and loss of voice, occasionally associated with difficulty breathing, are signs of laryngeal involvement.

EBA has been associated with other conditions, such as inflammatory bowel disease (IBD), including ulcerative colitis and Crohn's disease. The linkage between IBD and EBA has been demonstrated in both, human and animal models. Firstly, IBD has been reported in 30% of EBA patients and patients with IBD have been found to present anti-CVII IgG with frequencies ranging from 6 to 60%. Secondly, IBD is consistently developed in EBA animal models, in which blister formation is not limited to the skin, involving also esophagus (40% of mice), stomach (40% of mice), small intestine (20% of mice) and colon (20% of mice), with the functional consequence of weight loss (21). Other anecdotal associations have been described with diabetes mellitus, psoriasis, cryoglobulinemia, amyloidosis, rheumatoid arthritis, pulmonary fibrosis, chronic lymphocytic leukemia, thymoma and subacute cutaneous/systemic lupus erythematosus, among others (11, 12).

### *2.c.iii. Diagnosis*

EBA is difficult to diagnose because of its rarity. Table 2 shows the criteria for its diagnosis as summarized by Gupta *et al* (12). Moreover, in order to perform the specific indicated work up, it requires a high suspicion by physicians, and some of the diagnostic tests are not always available per standard of care in all health care centers. By definition, EBA diagnosis requires the following criteria: presence of tense blisters in mucocutaneous areas plus the detection of circulating autoantibodies against CVII, as well as tissue deposition of anti-CVII antibodies along the BMZ. The common work up performed in these patients includes: 1) skin biopsy which shows a dermal-epidermal disruption with variable inflammatory infiltrate (normally neutrophils if it corresponds to an inflammatory form of EBA); 2) demonstration of deposition of antibodies, usually immunoglobulin (Ig) G, on the BMZ, by direct immunofluorescence (DIF) study, while IgA can also be occasionally seen; 3) demonstration of circulating antibodies against CVII by either indirect immunofluorescence (IIF), enzyme-linked immunosorbent assay (ELISA), or Western-blot.

*Skin biopsy.* Early lesions show papillary edema and vacuolization of the basal layer, while at later stages subepidermal blister is the main feature. The degree, location and composition of the dermal granulocytic infiltrate are variable, although it is normally present around vessels, follicles, and also scattered within the interstitium. Different histologic features have been investigated to potentially differentiate one clinical subtype from another. A sparse infiltrate is typically seen in the classical form of EBA. In contrast, the BP-like form shows a moderate infiltrate with admixture of neutrophils, monocytes and eosinophils, making it difficult to differentiate it from BP itself. As a matter of fact, histopathology by itself cannot lead to a diagnosis of EBA, and further testing is required with DIF, IIF, ELISA, immunoblot or other more complex immunobiochemical studies.

*DIF.* Patient's skin biopsy is exposed to antibodies that are marked with fluorescein isothiocyanate (FITC) and have affinity to the constant fragment (Fc) of human antibodies. Thus, when positive, it demonstrates the deposition of the patient's antibodies on the

BMZ, yet the specific target cannot be identified. The characteristic pattern is consistent with a linear deposition along BMZ of IgG and/or IgA. It is positive in at least 93% of EBA patients, and negative in the remaining 7%. Thirty-nine percent are IgG positive, 19% are IgA positive and 35% have deposits of both Ig types. Interestingly, cases with ocular involvement are related to IgA autoantibodies. More precisely and almost exclusive of EBA, this linear deposition of the antibodies has been better described as u-serrated pattern (following the anchoring fibrils architecture at the BMZ), compared with an n-serrated pattern described in bullous pemphigoid among others subepidermal blistering diseases (Figure 1). This pattern can be read with a conventional microscope at x40 objective, but requires a trained of the observer (22, 23).

III.F. This method exposes autoantibodies from the patient's serum to other tissues of human or other species origin (e.g. human foreskin, monkey esophagus, rat bladder, rabbit lip, etc.). When using human skin as a substrate, this test has a higher sensitivity when the tissue has been previously incubated with 1 molar sodium chloride solution (also called *salt-split skin test*), where dermis and epidermis are chemically separated along the lamina lucida, and thus, antigens become more widely exposed at both the roof and floor of the artificially-induced blister. Deposition of antibodies from patient's serum to the floor of the dermal-epidermal separation is highly suspicious of EBA, yet not confirmatory, as other autoimmune blister conditions such as anti-p200 pemphigoid, can also present the same pattern.

ELISA. The purpose of the test is to detect circulating antibodies against a specific target. By coating fragments from different non-collagen (NC) domains of CVII (NC1 only, as most of the patients have antibodies only against to this domain, or NC1 plus NC2) on a plate and incubating with patient' sera, the presence of antibodies can be detected by an enzymatic reaction that induces a visible signal, which correlates with the amount of antibodies. It is an attractive technique, as it is a confirmatory test of the disease when clinical features are present, with a sensitivity and specificity of >90%, and this is nowadays commercially available (9, 24, 25).

Immunoblot. Western-blot using dermal extracts has been the technique of choice for several years in order to confirm EBA. Similar to ELISA, it also detects the presence of autoantibodies in the patient's serum against a 290-kDa protein, which corresponds to the molecular weight of CVII. However, this technique requires time, and it is not normally available in most health care centers. Thus, it is less commonly used as part of the standard work up.

Other diagnostic tests. Transmission electron microscopy (TEM), immunoelectron microscopy (IEM), and fluorescent overlay antigen mapping (FOAM) are other ancillary studies, without any direct benefit to patient care, but performed for research purposes. TEM, the routine electron microscopy, reveals a decreased number of anchoring fibrils in the lamina densa, and blister formation situated in the dermis leaving the basal lamina in the roof of the blister (11, 26-28). IEM shows the presence of immune deposits in the anchoring fibril zone at the lamina densa, which is unique compared to other autoimmune blistering diseases. Finally, FOAM differentiates location of the immune deposits by staining the antigen and antibodies in the same skin biopsy. It is less expensive, easier to analyze and quicker than IEM (11, 28).

**Table 2.** Diagnostic criteria of EBA (12).

| <b>Diagnostic criteria</b>   |
|--|
| <ol style="list-style-type: none"><li>1. Bullous skin disorder</li><li>2. Lack of family history of a bullous disorder</li><li>3. Histology revealing a subepidermal blister</li><li>4. A positive DIF of perilesional skin showing deposition of IgG deposits within BMZ</li><li>5. IEM of perilesional skin indicating localization of IgG deposits within the lower lamina densa and /or sublamina densa zone of the BMZ</li><li>6. Alternative laboratory tests for item 5 include indirect or direct salt-split skin immunofluorescence, IIF using substrate deficient in basement membrane molecules, Western blotting, FOAM, and ELISA; however, a salt-split skin immunofluorescence may not be conclusive in the differentiation of true MMP from EBA when clinical presentation is MMP-like.</li></ol> |

### 2.c.iv. Treatment

Treatment of EBA patient is challenging, due to the chronicity and refractoriness of the disease, which often makes its management frustrating for both, physicians and patients. These patients require two main approaches: 1) immunosuppressive drugs including systemic glucocorticoids, as well as glucocorticoids-sparing agents and monoclonal antibodies (such as rituximab); and 2) supportive care to reduce complications such as wound infections and to improve patients' quality of life (the latter is no longer mentioned in this thesis as a marginal issue).

Efficacy of each drug is difficult to assess as the rarity of the condition does not allow performing controlled blinded randomized clinical trials. Since the aim of the thesis is reviewing pathophysiology of EBA, a summary of each drug by mechanism of action is presented below (Table 3).

**Table 3.** Mechanism of action and adverse events of the current therapy used in EBA (11, 29-35).

| Agent                  | Mechanism of action   | Adverse events  | Comments   |
|------------------------|---|---|--|
| <b>Glucocorticoids</b> | Immediate effects: inhibition of vasodilation.<br>Late effects: Block the expression of pro-inflammatory genes and induce transcription of anti-inflammatory agents | Cushing's syndrome<br>diabetes mellitus,<br>osteoporosis,<br>avascular necrosis of the femoral head,<br>cataracts, peptic ulcer, hypertension, acne | Main treatment for most of the EBA patients. Normally given initially to control severe disease. |
| <b>Colchicine</b>      | Inhibits neutrophils mobility and chemotaxis, interfering with the microtubules; decrease Ig secretion by plasma cells  | Diarrhea, bone marrow suppression, myopathy, urticaria, toxic epidermal necrolysis  | Given as monotherapy in mild cases of EBA, it is considered first line treatment                 |
| <b>Dapsone</b>         | Not well understood. It is thought to the blockade of reactive oxygen species synthesis   | Hemolytic anemia, agranulocytosis, methemoglobinemia, peripheral  | It has been reported in several case reports and occasionally as                                 |

|  |   |  |   |
|--|---|--|---|
|  |   | neuropathy, headache, vertigo  | monotherapy   |
| <b>Cyclosporine</b>                          | Inhibits T-cell activation through inhibiting transcription of IL-2   | Nephrotoxicity, hypertension, diarrhea, hyperkalemia, hypomagnesemia, hyperuricemia and hyperlipidemia, hypertrichosis | Case reports, however not usually indicated   |
| <b>Methotrexate</b>                          | Inhibits dihydrofolate reductase interfering with <sup>b</sup> DNA synthesis  | Myelosuppression, nausea, vomiting, myelosuppression, hepatotoxicity, pulmonary toxicity                               | Never used as monotherapy   |
| <b>Azathioprine</b>                          | Interferes with the synthesis of purines ( <sup>b</sup> DNA synthesis)  | Bone marrow suppression, macrocytosis, nausea, vomiting, hepatitis, pancreatitis                                       | Never used as monotherapy.  |
| <b>Mycophenolate mofetil</b>                 | Inhibits inosine monophosphate in the purine synthesis ( <sup>b</sup> DNA synthesis)  | Gastrointestinal upset, bone marrow suppression, infections, weakness, tiredness                                       | Adult and pediatric case reports  |
| <b>High dose intravenous immunoglobulins</b> | Unclear, increase clearance of antibodies, direct inhibitory effect on T- and B-cells functions   | Headache, acute renal failure, aseptic meningitis, migraine, flu-like symptoms, hypotension, chest tightness           | Used as second line therapy in refractory disease. Long-term use as monotherapy once response is achieved.        |
| <b>Plasmapheresis</b>                        | Removal of antibody from blood  | Infections, hypotension, transfusion reactions, bleedings  | Greater experience with pemphigus, limited experience in EBA  |
| <b>Rituximab</b>                             | Monoclonal antibody against CD20 (B-cell lymphocytes), avoiding development of plasma cells   | Infusion reaction, hepatitis B reactivation, opportunistic infections, progressive multifocal leukoencephalopathy      | Wide experience in pemphigus. Phase III clinical trial for pemphigus. EBA only used in a limited number of cases. |
| <b>Extracorporeal photochemotherapy</b>      | Monocytes with maximal exposure to 8-methoxypsoralen develop into short-lived immature <sup>a</sup> DC with anti-inflammatory responses | Hypotension, syncope   | Case reports  |



|                         |   |   |   |
|-------------------------|---|---|---|
| <b>Immunoadsorption</b> | Removal of antibody from blood                      | Rare  | Rapid onset response, limited use in EBA, widely used in Pemphigus patients |
| <b>Cyclophosphamide</b> | Alkylating agent, cross-linkage of <sup>b</sup> DNA | Leukopenia, hemorrhagic cystitis, infertility, hepatotoxicity, malignancy | Rarely used in EBA  |

<sup>a</sup>DC: dendritic cells; <sup>b</sup>DNA: deoxyribonucleic acid

The current therapies presented above show a broad spectrum of mechanisms of action and are also notable for multiple side effects. Furthermore, infusion therapies require a well equipped-facility plus patient's schedule availability to receive appropriate treatment at the health care center. Therefore, significant research efforts are focused on developing a target therapy for EBA, with less side effects, and easier administration of the drug to the patient. Future potential drug candidates are presented in Table 4 with their mechanism of action.

**Table 4.** Possible future therapies for EBA (11, 36-40).

| <b>Agents</b>                                     | <b>Mechanism of action</b>   | <b>Evidence</b>   | <b>Other conditions where it has been investigated</b>                                      |
|---|--|---|---|
| <b><sup>a</sup>Hsp90 inhibitors</b>               | Inhibits antibody production by targeting autoreactive T-cells.                                      | Prevented onset of antibody-transfer-induced EBA, and improved already established immunization-induced EBA | Phase I-II for multiple myeloma. Several adverse effects, including death-related treatment |
| <b>SM101, soluble <sup>b</sup>FcγRIIB</b>         | Blockade <sup>b</sup> FcγR, which is a key feature for autoantibody blister formation                | Potential candidate.  | Phase II for primary immune thrombocytopenia, and systemic lupus erythematosus              |
| <b>Natalizumab</b>                                | Anti-α4 integrin, modulates leukocyte extravasation  | Potential candidate. No literature evidence   | Used in multiple sclerosis. Cases with progressive multifocal leukoencephalopathy           |
| <b>Efalizumab</b>                                 | Anti-CD11a, inhibits leukocyte extravasation   | Not successfully controlling skin inflammation  | It has been withdrawn for psoriasis   |
| <b>Anti-<sup>c</sup>CCR4 (KW-0761)</b>            | Inhibits leukocyte recruitment into the skin   | Non-tested in skin inflammatory conditions  | Used for relapse adult T-cell leukemia lymphomas, cutaneous T-cell lymphoma                 |
| <b>Modified heparins (<sup>d</sup>PS3)</b>        | Targets disruption of leukocyte extravasation  | Has demonstrated anti-inflammatory and antimetastatic effect  | It has less anticoagulant effect than heparin itself  |
| <b>Reparixin or <sup>e</sup>CXCR1/2 inhibitor</b> | Inhibits neutrophil chemoattractant activity   | Prevented onset of antibody-transfer-induced EBA, and improved already established immunization-induced EBA | Phase II for pancreatic islet transformation  |
| <b>Blockade of <sup>f</sup>GM-CSF</b>             | Inhibits colony stimulating factor of granulocytes, decrease antibody formation and neutrophil count | Beneficial in antibody transfer- and immunization-induced EBA.  | Phase I-II for Rheumatoid arthritis   |
| <b>Anakinra</b>                                   | Partial modulation of IL-6, which has anti-inflammatory effect                                       | Potential candidate. Never used in EBA.   | Used effectively in Schnitzler's syndrome   |

<sup>a</sup>Hsp: heat-shock protein; <sup>b</sup>FcγRIIB: receptor of the constant fragment of antibody; <sup>c</sup>CCR4: C-C motif chemokine receptor 4; <sup>d</sup>PS3: semisynthetic glucan sulfate; <sup>e</sup>CXCR1/2: C-C motif chemokine receptor 1/2. <sup>f</sup>GM-CSF: granulocyte macrophage colony-stimulating factor.

With all the treatments mentioned above, it seems that EBA patients have numerous treatment options, however none of these new molecules can fully or partially substituted for old treatments. Obviously, the efficacy of new agents is difficult to be tested and compared with other available treatments due to low prevalence/incidence of the disease. Thus, collaboration of multiple centers to increase study patient number is necessary in order to gather enough and significant data regarding efficacy as well as the drugs' adverse events. Table 5 shows the well-accepted current treatment regimens for EBA patients.

**Table 5.** Treatment suggested by EBA severity, defined as follows (41):

| <b>Mild EBA<br/>(&lt;5% of body surface area<br/>without mucous membrane<br/>involvement)</b>                               | <b>Moderate EBA<br/>(5 – 15% of body surface area<br/>and or two or more mucous<br/>membranes involvement, not<br/>including eyes)</b>  | <b>Severe EBA<br/>(Greater than 5% of body<br/>surface area or greater than<br/>two mucous membranes<br/>involved or ocular<br/>involvement )</b> |
|---|---|---|
| Oral steroids (0.5 – 1 mg/kg/d)<br>+<br>Colchicine 0.5 – 1 mg/d (mild) or 1-3 mg/d (moderate)<br>±<br>Dapsone 1 – 2 mg/kg/d | Oral steroids (0.5 – 1 mg/kg/d)<br>+<br>Colchicine 1-3 mg/d<br>(moderate)<br>±<br>Dapsone 1 – 2 mg/kg/d<br>±<br>IV steroids pulse<br>±<br>Mycophenolate mofetil 1 – 2<br>g/d<br>±<br>Plasmapheresis<br>±<br>IVIG 1 – 2 g/kg over 3 – 5 every<br>4 weeks<br>±<br>Rituximab 375 mg/m <sup>2</sup> /wk for<br>4 wk |   |

Although EBA is a rare condition, our extensive knowledge of its pathophysiology and immunology are intriguing and offer the unique opportunity to investigate methods to improve diagnosis and treatment options with the objective to improve patient's quality of life.

#### *2.d. Experimental models of EBA*

A summary of experimental models of EBA is presented in Table 6.

##### *2.d.i. Ex vivo*

There are two *ex vivo* experimental models described in the literature: the cryosection model and the regenerated/organ cultured human skin.

The former has been comprehensively characterized compared with the latter. The cryosection model technique takes human skin (normally neonatal foreskin) and exposes it to patient's serum, which is further incubated with leukocytes from healthy donors.

The same process is used for the regenerated/organ cultured human skin technique, although the substrate to expose patient's antibodies is cultured skin. Both techniques directly demonstrate the pathogenicity of anti-CVII IgG in EBA patients, yet the organ culture model has not further been used (42).

##### *2.d.ii. In vivo*

Two types of animal models have been described, the so-called passive and active models. Passive-transfer experimental models are those where the disease is induced by the injection of antibodies against the target protein, whereas in active models, animals develop the disease by immunization with the target antigen, this is, by injection of the

target protein or peptide. Therefore, in the active model, animals do produce their own pathogenic antibodies in response to the artificial immunization with an antigen.

*Passive-transfer animal model of EBA.* There are two types of passive transfer animal models of EBA, in which the source of antibodies differs one from the other. One is the rabbit IgG anti-CVII passive transfer animal model, in which antibodies come from immunized rabbits with human or murine fragments of CVII. And the second is the human IgG anti-CVII, in which antibodies come from EBA patients after plasma has been purified and concentrated.

*Passive transfer of rabbit IgG against CVII.* Inbred mouse strains such as BALB/C, C57BL/6 and outbred mice SKH-1 developed EBA phenotype after the subcutaneous injections of the antibodies. Protocol consisted of the injection of antibodies every other day for a total of 40 – 90 mg in six divided doses. The first lesions were seen 2 to 4 days after the first dose of antibody, and full-blown disease, meaning the presence of erythema, blisters and crust associated with alopecia, was seen 5 to 6 days after the first injection. Moreover, disease extension correlated with the total IgG dose. After 12 days, mice were sacrificed. Skin biopsies showed histological findings typically described in human EBA, with a mixed inflammatory infiltrate rich in neutrophils, along with dermal-epidermal separation. DIF of mice skin biopsies showed a linear deposition of rabbit IgG at the BMZ, as well as linear deposition of mouse C3 at the BMZ. ELISA of mice sera extracted each day or every other day revealed increasing levels of IgG (42, 43).

*Passive transfer of patients' IgG against CVII.* The development of blisters by the passive transfer of autoantibodies from EBA subjects to SHK-1 mice clearly demonstrates the pathogenicity of the autoantibodies. However, the high amounts of human antibodies that are needed to induce the disease phenotype make this type of animal model impractical. This is due to two facts: first, EBA patients are exceedingly rare, and second, it seems that human IgG antibodies from EBA patients show low affinity for mice Fc gamma receptors. In short, these are the reasons why most authors use rabbit antibodies

after immunizing them with murine collagen VII peptides, instead of EBA patients' sera (43-45).

Active disease model of EBA. In these models, disease phenotype is achieved by immunizing the animals by means of the injection of certain fragments of recombinant murine CVII associated with an adjuvant (usually a non-ionic block copolymer, or other adjuvant such as CpG, pertussis or cholera toxins). It requires repeated injections of the antigen (at least two to three times) at 3-week intervals for a total of 12 weeks, to achieve full-blown disease. Inbred mice, including BALB/C, and outbreed such as SJL-1, AJ are able to develop an immune response after injection of the murine CVII. Interestingly, the genetic background is strongly associated with the susceptibility for disease development. For instance, SJL-1 mice have an incidence of 80 to 100%, whereas only 50% of the BALB/C mice develop the disease phenotype. Thus, outbreed SJL-1 is the preferred strain for this type of animal model. This active model is useful to dissect the cellular and molecular aspects of pathogenic autoantibody production, and to design immunomodulatory treatments for EBA (42, 46).

**Table 6.** Summary of experimental models of EBA (42).

| Type of experimental model       | Source                      | Phenotype induced by   |
|----------------------------------|-----------------------------|--|
| <b>Cryosection model (47)</b>    | Human neonatal foreskin     | anti-CVII IgG from EBA patients, incubated with human leukocytes from healthy donors |
| <b>Skin organ culture (48)</b>   | Regenerated human skin      | anti-CVII IgG from EBA patients, incubated with human leukocytes from healthy donors |
| <b>Passive transfer (45, 47)</b> | BALB/C, C57BL/6, SHK-1 mice | Rabbit or murine anti-CVII IgG or human IgG from EBA patients                        |
| <b>Active model (46)</b>         | Preferably SJL-1 mice       | Murine CVII associated with antigenic adjuvant                                       |



### **3. BACKGROUND**

---





### **3. BACKGROUND**

The pathogenesis of EBA is still unclear even though the role of the autoantibodies seems to be crucial in the development of the disease. EBA is genetically associated with the MHC class II haplotype, in particular HLA-DR2, HLA-DRB1\*15 in blacks and HLA-DRB1\*13 in Koreans (9, 13-15, 49, 50). Overall, EBA pathogenesis can be summarized in three consecutive steps; 1) loss of tolerance against CVII; 2) maintenance of antibody production once loss of tolerance to anti-CVII has been established; and 3) the tissue injury triggered by the deposition of autoantibodies at the BMZ (11, 51, 52).

In order to cover the pathogenesis of EBA, this section will discuss the structure and function of CVII as a protein and target antigen, the loss of tolerance to CVII by autoreactive T-cells, and the phenomena involved in the development of tissue injury. The latter corresponds to the focus of this doctoral thesis.

#### *3.a. Type VII collagen*

The COL7A1 is the gene encoding the CVII protein, which contains two main domains: collagenous and non-collagenous. The collagenous domain is formed by a triple helical structure containing repeating glycine-proline-hydroxy proline or hydroxyl lysine (Gly-X-Y) sequences. The non-collagenous (NC) domain can be divided as follows; 1) a 39-amino acid domain forming the hinge region located in the center of the collagenous domain; 2) an N-terminal domain of 145 kDa, also called NC1; and 3) a C-terminal domain of 34 kDa, also known as NC2. NC1 domain has subdomains that are structurally similar to other proteins with adhesion function such as cartilage matrix protein, nine fibronectin III-like domains and von Willebrand factor A-like domain followed by a cysteine and proline-rich domain (11, 53, 54). NC2 domain is structurally similar to protease inhibitor molecules.

The CVII protein is organized as follows: headed by an N-terminal 145 kDa NC domain, followed by a triple-helical of collagenous domain disrupted by a NC hinge region in the

center, and terminated with a C-terminal 34 kDa domain. When CVII is released by the fibroblast to the extracellular matrix, NC2 domain is cleaved, and then two identical CVII proteins align tail-to-tail to form a dimer linked by disulfide bonds. This structure corresponds to the anchoring fibrils that are attached to different proteins of the lamina densa of the BMZ. Specifically, fibronectin III-like domains bind to laminin 332, von Willebrand factor A-like domains bind to collagen I; however, the specific NC1 subdomain where collagen IV binds remains unknown (Figure 2) (55-57).

In the setting of an autoimmune condition, it is of interest to search for the specific areas of the protein that induce more antigenic reaction than other regions. A second interest is to determine the capability of those antibodies to induce disease. These have been well characterized in EBA. First, the antigenicity of CVII in the setting of EBA patients has been studied by epitope-distributed mapping. The major number of epitopes is located in the NC1 domain, though antibodies against the collagen domain and NC2 have also been described with less frequency (58-64). Second, the pathogenic relevance of the antibodies against CVII has been demonstrated not only *ex vivo* (by cryosections), but also *in vivo* by inducing EBA in mice with the passive transfer of rabbits' and patients' autoantibodies (mentioned in *Experimental animal model* section). A relationship between the different epitopes recognized and the different phenotypes of the disease (e.g. mechanobullous, inflammatory) could not be demonstrated (43, 45, 65). Currently, and as discussed above, the disease severity has been shown to correlate with the level of circulating antibodies (19).

Upon characterization of the most antigenic areas of CVII and demonstration of the pathogenicity of antibodies, a comparison of disease severity between the different epitope-specific antibodies was performed in a passive transfer animal model (66). By a functional epitope mapping with antibodies against different fragments of NC1 and NC2, it was shown that autoantibodies against NC2 domain do not induce blistering skin disease, which is in contrast to the antibodies against. The authors suggested a low specificity of the IgG against the NC2. Therefore, a higher amount of IgG was required to

induce disease, which probably caused at the same time, a saturation of the neonatal Fc receptor (which participates in hemostasis of immunoglobulins) and favored their catabolism. Thus, pathogenic relevance of NC2 still needs to be elucidated. On the other hand, mice injected with specific antibodies against epitopes located on the amino acids (aa) 281 to 1125 of the NC1 domain showed more severity of the disease compared with those mice that received antibodies against epitopes located on the aa 26 – 300 or 1108 – 1323 of NC1 (66). For this reason, fragments of human or murine NC1 domain localized on the aa 281 to 1125 are used in the experimental animal models to induce either disease in active animal model, or antibody formation for passive transfer animal models. In this research project, we specifically used a reviewed fragment located in aa 759-980, named as fragment C of the murine CVII (mCVIICr).

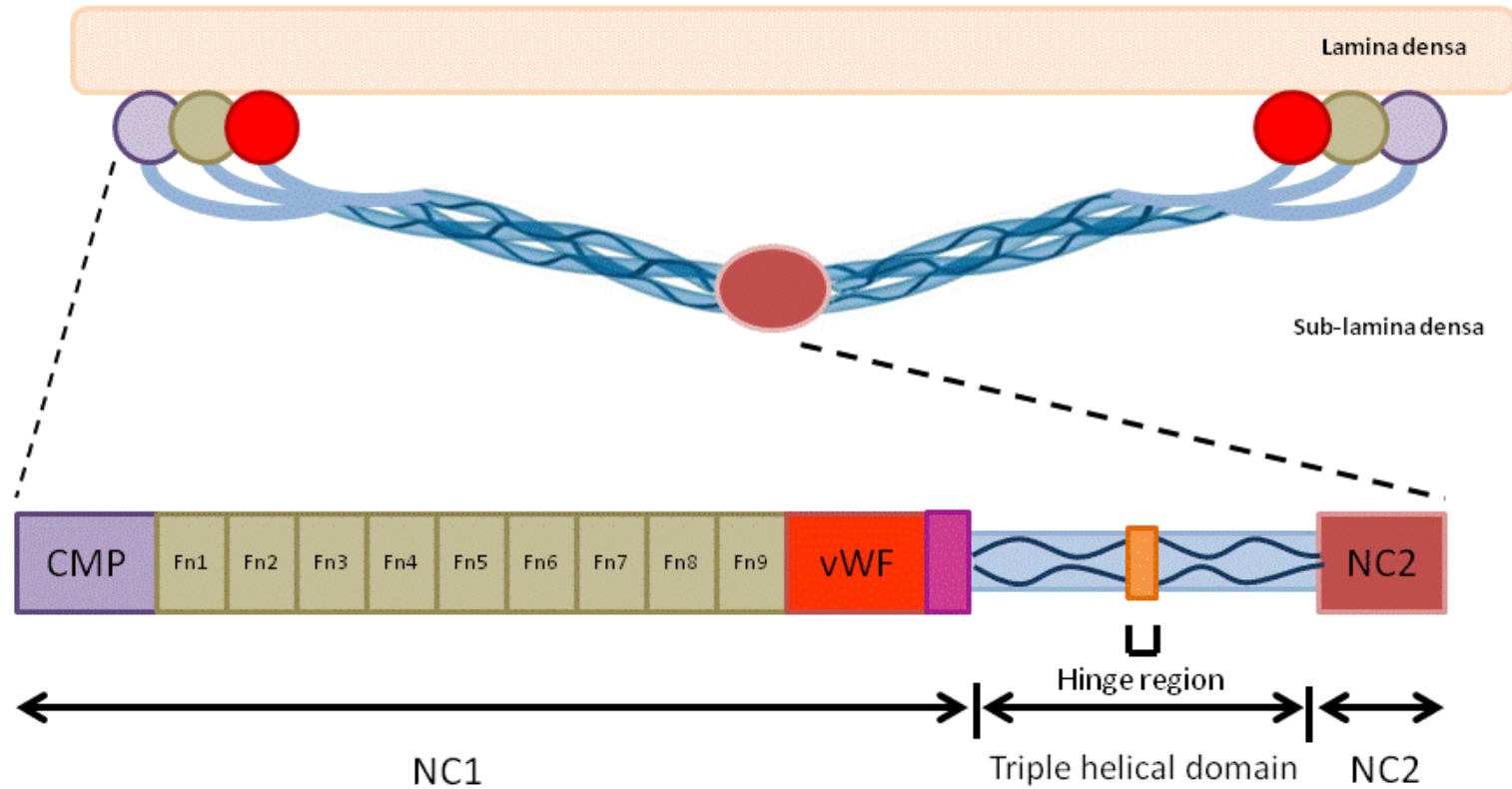


**Figure 2. Type VII collagen.** Headed by NC1 domain (N-terminal), followed by a triple-helical of collagenous domain disrupted by a NC hinge region in the center, and terminated by NC2 (C-terminal). NC2 domain is cleaved at the extracellular matrix, and then two identical CVII proteins align tail-to-tail to form a dimer linked by disulfide bonds. This structure corresponds to the anchoring fibrils that are attached to different proteins of the lamina densa of the BMZ. Specifically, fibronectin (Fn) III-like domains bind to laminin 332, and von Willebrand factor (vWF) A-like domains bind to collagen I. CMP: cartilage matrix protein (9).

### 3.b. Loss of immunological tolerance

The mechanism in which T or B-cells react against self-antigens is known as loss of tolerance. This implies two steps throughout disease course, first its development and second its maintenance. The latter favors the chronic nature of the disease. Autoantibodies are the B-cell product generated from this mechanism and they can be developed directly from autoreactive B-cells or indirectly from autoreactive T-cells interacting with B-cells. It has been shown, that T-cell-deficient mice cannot develop EBA phenotype by active immunization (induction of autoimmune response in experimental animal model). Yet, EBA is clinically induced when the T-cell population is restored in these mice (11, 67). In addition, autoreactive T-cells against the same epitopes of CVII targeted by IgG autoantibodies have been demonstrated (51, 68). Further studies have characterized those T-cells as CD4<sup>+</sup> T-cells. However, the type of antigen presenting cell that favors the clonal selection and expansion of the CD4<sup>+</sup> T-cell remains unknown (11, 51, 67).

Neonatal Fc (*fragment crystallizable*, constant fragment of the antibody) receptor is a subtype of Fc receptor that functions to transport mother's IgG through the placenta, but also monitors IgG homeostasis. Once loss of tolerance has been developed, neonatal Fc receptor plays a major role in controlling serum levels of IgG against CVII, thus maintaining the autoimmune response, and so, the maintenance of disease. Indeed, mice deficient in neonatal Fc receptor were protected from EBA induction (52).

Heat-shock proteins (Hsp) are a family of proteins that are produced by cells in stressful conditions, initially related to heat shock, and latter detected in other stressful conditions such as wound healing. An inhibitor of Hsp subtype 90 (Hsp90) has been shown to induce death of malignant plasma cells (for instance, in multiple myeloma). Kasperkiewicz et al. raised the question whether if this inhibitor could also target non-transformed plasma cells. Surprisingly, in EBA, Hsp90 inhibitor was found to target T-cell proliferation. By the administration of Hsp90 inhibitors in passive transfer animal model or active animal model, mice did not developed disease, or presented with milder severity of EBA.

Moreover, in the active animal model, a decrease of B-cell proliferation was detected, yet no impact was seen in autoreactive plasma cells (69, 70).

### *3.c. Tissue injury*

Different clinical phenotypes of EBA may result from different mechanisms of tissue injury. As discussed above, in broad terms there are two types of clinical presentation of EBA, inflammatory and mechano-bullous (non-inflammatory). In the mechano-bullous EBA subtype, a reduction in the number of anchoring fibrils is seen in either lesional and perilesional skin has been described, along with a scattered inflammatory infiltrate. It is suspected that the direct effect of the antibody disrupts the joining of anchoring fibrils to the lamina densa and the formation of the antiparallel dimer (71). As a matter of fact, the pathogenesis of mechanobullous EBA is very difficult to investigate as all the experimental animal models mimic the inflammatory form of EBA.

On the other hand, the innate immune system seems to play a major role in the inflammatory form of EBA (the most frequent presentation in humans), triggered by the autoantibodies bound to the dermal-epidermal BMZ. Overall, it consists on a complex pathway with activation of multiple elements that subsequently induces tissue injury. A disruption of this complex pathway seems to be the main target for the development of new and more specific therapies. Among others, possible therapeutic targets include the Fc (constant fragment of autoantibodies) or its receptors, alternative complement pathway, neutrophils and the generation of reactive oxygen species (ROS). As mentioned above, each distinct types of experimental EBA animal models represent the inflammatory clinical phenotype, which results in reliable reproduction of the inflammatory environment occurring in EBA (9).

### *3.c.i. Role of the complement system*

The alternative complement pathway is the part of the innate immune system that participates in opsonizing and killing pathogens through the membrane attack complex. Specifically, complement 5a (C5a), a component of the alternative pathway, is a potent leukocyte chemoattractant. Passive transfer of antibody against CVII in C5-deficient mice failed to induce experimental EBA (9, 43, 51). Further studies with mice that received passive transfer of IgY (chicken immunoglobulin -by itself incapable to activate murine complement-) against CVII did not developed experimental EBA (72). In contrast, mice deficient in classical pathway (C1q) or mannose binding lectin-complement components showed the same severity in EBA phenotype compared with wild type mice with the passive transfer of antibodies against CVII (73).

The synthesis of this information reveals, it is agreed that the alternative complement pathway is an important key factor in the EBA pathogenesis. However, its role is more important as an intermediate factor by recruiting neutrophils than a direct toxic effect on the skin. The latter is shown by the fact that *ex vivo* dermal-epidermal separation is induced by autoantibodies when incubated with granulocytes on cryosections of normal skin, where complement is absent.(51).

### *3.c.ii. Neutrophils*

With the attachment of antibodies and activation of complement, neutrophils are recruited to the skin, which are considered as the most significant cells in tissue injury. There are still some controversies regarding this statement. First, inhibition of colony-stimulating factor (CSF), specifically granulocyte-macrophage(GM)-CSF (Csf2) that is the most potent with regards to the recruitment of neutrophils and macrophages to sites of inflammation, showed reduced skin blistering in a rabbit IgG anti-CVII passive transfer animal model. Moreover analysis of the immunization-induced epidermolysis bullosa acquisita animal model on GM-CSF KO mice, lower serum autoantibody titers suggesting,



that GM-CSF also modulates antibody production (74). This phenomenon has already been shown in other conditions, where antibody generation is modulated by B cell helper neutrophils. Another example is the contribution of GM-CSF to the formation of anti-influenza IgG (40, 74). Anti-Gr1 is a monoclonal antibody that mainly depletes neutrophils and monocytes. The injection of this monoclonal antibody showed protection in the experimental antibody induced-EBA. However, the fact that anti-Gr1 can also deplete monocytes questions the theory that tissue injury is limited to neutrophils (51, 75, 76).

Another finding suggesting the neutrophil involvement in tissue injury was the involvement of IL-8 (which corresponds to CXCL-1 and CXCL-2 in mice). IL-8 is known to induce neutrophil chemotaxis and phagocytosis. It was shown that they are (CXCL-2>CXCL-1) are highly expressed in the mice's skin when EBA is induced. Moreover, skin blistering is not observed by blocking their receptors. More evidence of the neutrophil involvement is the release of ROS and proteolytic enzymes (such as metalloproteases and elastases), which finally induce blister formation and will be further examined in section 3.c.iv.

### *3.c.iii. Fc receptors*

Fc receptors (FcR) have recently been an important target in the field of EBA research. These receptors are localized on the surface of cells (e.g. neutrophils, macrophages, natural killer cells) and have different mechanisms of action including facilitating antigen presentation, inducing phagocytosis or antigen-dependent cellular cytotoxicity, and releasing toxic oxygen metabolites and inflammatory mediators.

There are different subtypes of FcR that correspond to each subclass of the immunoglobulins. For instance Fc $\gamma$ R binds to IgG, Fc $\epsilon$ R to IgE, and Fc $\alpha$ R to IgA. Focusing on IgG, there are also different subtypes of Fc $\gamma$ R with the aim of modulating the immune response, meaning that there is no exclusive activation or inhibition of the immune response, yet there is balance between both immune responses (77). In normal conditions, this protects against an exaggerated immune response as inhibitory function

would balance activator response. This activator or inhibitor function is defined by two types of receptor-associated signal-transducing molecules, such as immunoreceptor tyrosine-based activation (ITAM) and inhibition motif (ITIM). ITAM is attached to activating receptors such FcγRIA, FcγRIIA and FcγRIIIA, and ITIM is bind to the inhibitory receptor FcγRIIB.

The role of FcγR in EBA tissue injury was demonstrated as follows. By removing the Fc portion of IgG with pepsin, the injection of the isolated variable portion of the antibody F(ab)2 with affinity to CVII showed no induction of EBA lesions in mice. And again, the injection of IgY that lacks affinity for murine Fc receptors did not show induction of blisters in mice (43, 78).

Recently, Kasperkiewicz et al. showed the exclusive importance of murine FcγRIV (which corresponds to the orthologue of human FcγRIIIA) for the tissue injury in EBA, among all others subtypes of FcγR. By gene expression profiling and weighted gene co-expression network analysis, they assessed the expression of FcγRIV using quantitative reverse transcription and polymerase chain reaction in the skin of wild type mice after treatment with pathogenic IgG. They found 1) an increased expression of FcγRIV and to a lesser extent expression of all the other FcγRs in murine skin biopsies, 2) a strong expression of FcγRIIIA in two out of three of human skin biopsies of EBA patients, and 3) weak expression of FcγRIIIA in control specimens or in EBA samples with scattered infiltrate (79). Thus, FcγRIV is considered as the important activator factor in the immune response (basically neutrophil activation) to develop tissue injury on EBA patients.

### *3.c.iv. Reactive-oxygen species*

Nicotinamide adenine dinucleotide phosphate (NADPH) oxidase is an enzyme complex located at the cell surface of neutrophils or in the membrane of the phagosome. It is composed of 6 subunits: a Rho guanosine triphosphatase (GTPase) usually Rac2, and five phagocytic oxidases (phox); gp91<sup>phox</sup>, p22<sup>phox</sup>, p40<sup>phox</sup>, p47<sup>phox</sup> (also called neutrophil

cytosolic factor 1), and p67<sup>phox</sup> (80). NADPH oxidase generates superoxide anion by transferring electrons from NADPH to the interior of the cell and coupling them to an oxygen molecule. Superoxide anion is a free radical that can spontaneously form hydrogen peroxide, which finally generates ROS. Deficiencies of NADPH in humans have been described to be due to a mutation in either gp91<sup>phox</sup> (X-linked) or p47<sup>phox</sup> (autosomal recessive), inducing chronic granulomatous disease (CGD) or Bridges-Good syndrome. Diagnosis is performed by the nitroblue-tetrazolium (NBT) test, where the lack of blue staining of neutrophils confirms an impairment of NADPH oxidase.

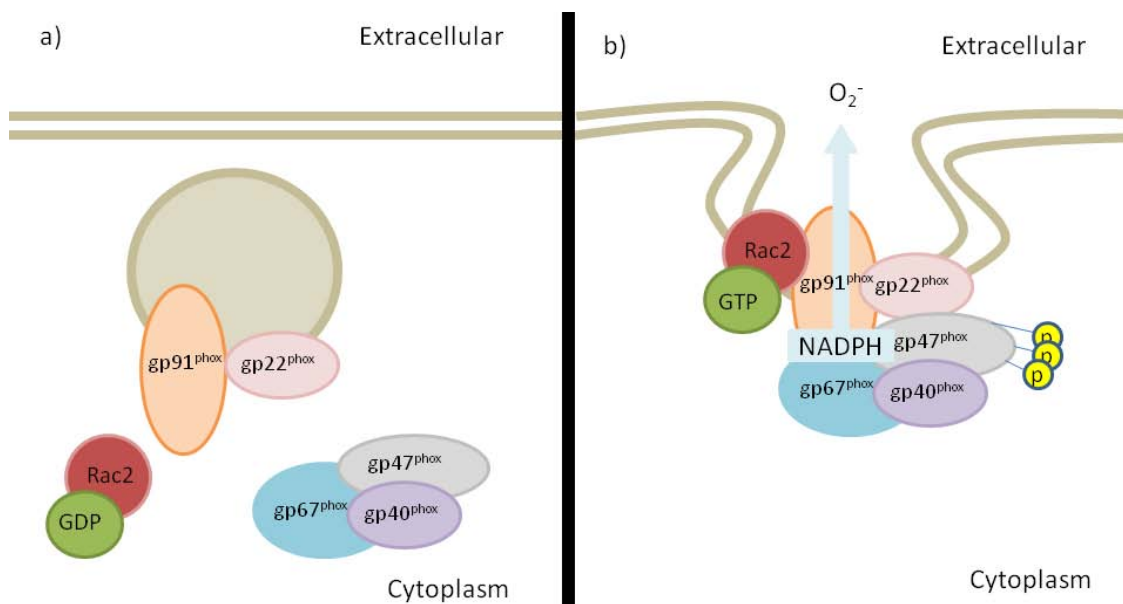


**Figura 3. NADPH oxidase complex.** a) Disassembled complex is present in the cytoplasm. b) Assembly of the complex and translocation to cytoplasmic membrane for the release of ROS (81).

The involvement of NADPH oxidase in EBA has been demonstrated by both *ex vivo* and *in vivo* experiments. The incubation of autoantibodies of EBA patients in cryosections of normal skin with neutrophils from patients with CGD showed no blue staining with NBT, confirming the absence of NAPH oxidase (76). Mice deficient in neutrophil factor 1 (p47phox) were also protected from developing EBA lesions with the injection of IgG against CVII (76). So, NADPH demonstrates an important role for tissue damaging in EBA patients, which makes this molecule of greatest interest as a target for therapies.

A summary of EBA pathogenesis is illustrated in figure 4.

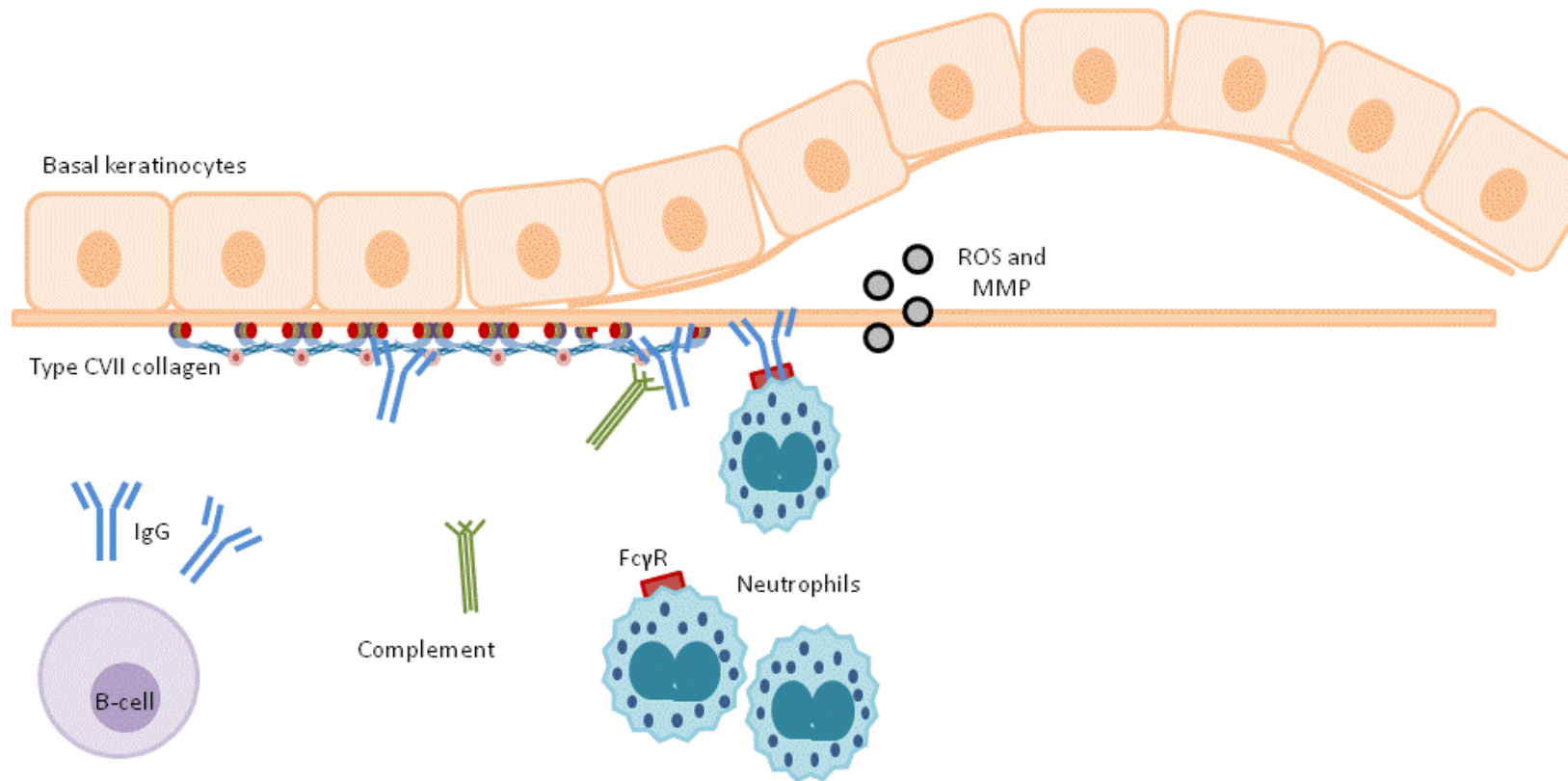


**Figure 4. Pathogenesis of EBA.** Tissue injury in EBA is developed as follows: 1) autoantibody binds to CVII at the dermal-epidermal BMZ through F(ab) fragments, 2) there is a complement activation that leads to recruitment of effector cells, including neutrophils, 3) Fc portion of the autoantibody binds to FcγRIV on immune cells causing their activation, and resulting with the release of ROS (by NADPH oxidase), serine and metalloproteases that mediate extracellular proteolysis (Courtesy of Dr. Sitaru, adapted image).

### *3.d. Rac2 protein*

As explained above, Rac2 protein is one of the subunits that form the complex of NADPH oxidase, although this protein has other functions of interest that might be important in EBA.

Rac2 (ras-related C3 botulinum toxin substrate 2) protein belongs to Rho GTPases, which are divided into families of proteins based on sequence homology, protein domains, and function. These include Rac, RhoA, Cdc42, TC10 and TCL, Rnd, the Rho BTB subset and the Miro subfamily. It is worth to mention, that Rho GTPases are subject to posttranslational modifications at the C-terminal sequence. The C-terminal sequence contains the CaaL sequence (C as cysteine, a as aliphatic aminoacid, and L as a Leucine), followed by a 'polybasic domain', in the majority of the protein of the Rho family. Posttranslational modifications consist in lipid modification and 'aaL' removal by proteolysis, which are critical in protein localization in the cell and its function (82).

The main functions of these proteins include cytoskeleton rearrangement, cell cycle progression and cell survival, cell adhesion, cell motility, cytokinesis and membrane trafficking, and regulation of gene transcription (82, 83). Focusing in the subfamily of Rac proteins, there are three types of Rac proteins encoded by different genes. Rac 1 is the most comprehensively studied and is ubiquitously expressed, while Rac2 is restricted to hematopoietic cells. These two isoforms share 92% identity and are highly homologous between murine and human species. Rac3 has been recently described and is less well characterized. It is also expressed in a variety of tissues and shares 72% and 83% identity with Rac1 and Rac2, respectively. It is important to remark that Rac2 protein differs from Rac1 in the polybasic domain at the C-terminal sequence. Rac2 protein contains only 3 basic residues compared to the polybasic residues present in Rac1. This non-polybasic domain gives unique functions to Rac2 protein (82, 84).

Rac proteins act as molecular switches that cycle between inactive (when associated to guanosine diphosphate (GDP)) and active (when associated to guanosine triphosphate (GTP)) states. Regulation of the active and inactive forms is mediated by: 1) Dbl-family

guanine nucleotide exchange factors (GEFs) that are activated by receptor-dependent kinases; 2) GTPases activating proteins (GAPs) that remove the phosphate and return the active GTPase to a GDP-bound (inactive) form of the protein; and 3) GDP dissociation inhibitors (GDIs) by sequestering or stabilizing the inactive form of the protein (82) (Figure 5).

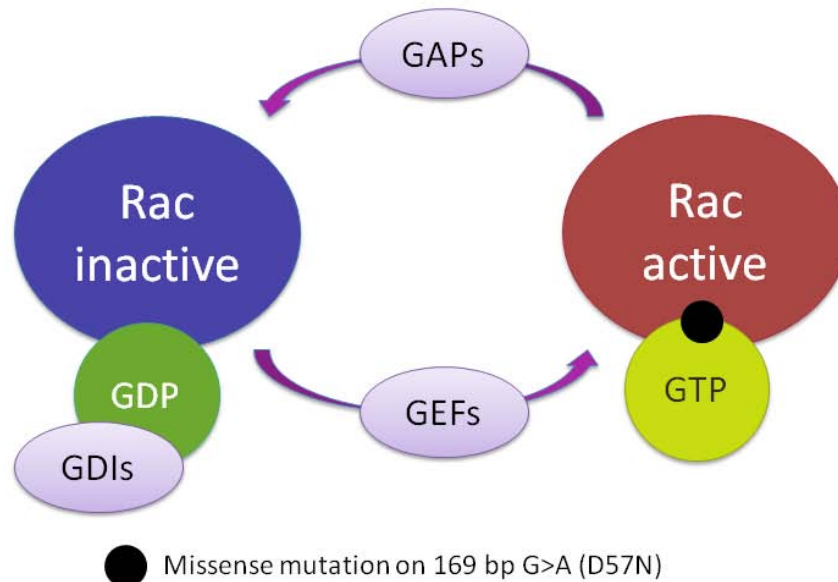


**Figure 5. Rac protein regulation.** Rac proteins cycle between inactive when associated to GDP-bound and active when associated to GTP-bound states. Regulation of the active and inactive forms is mediated by: 1) GEFs that are activated by receptor-dependent kinases; 2) GAPs remove the phosphate and return the active GTPase to a GDP (inactive) form of the protein; and 3) GDIs by sequestering or stabilizing the inactive form of the protein. The black dot shows the consequence of missense mutation found in human Rac2 deficiency disorder. GAPs: GTPase activating proteins. GEFs: guanine nucleotide exchange factor. GDIs: guanosine diphosphate dissociation inhibitors.

While Rac1/Rac2 proteins seem to play an important role in regulating the inflammatory response, Rac3 protein has been demonstrated to be more relevant in myelopoiesis. Further understanding of the Rac proteins function has been obtained after characterizing phenotypes of deficient mice for each isoform of Rac protein, differentiating their unique, as well as overlapping functions. For instance, it has been demonstrated that both Rac1 and Rac2 are required for functions related to the cytoskeleton (migration), and Rac2 was absolutely required for the activation of the NADPH oxidase, at least in mice (84, 85). Further studies on human neutrophils confirmed these results and specifically showed that Rac1 initiates migration towards the chemoattractant gradient, while Rac2 continues the migration and activation of NADPH oxidase on the target tissue. Another group studied the specificity regarding NADPH activation between Rac1 and Rac2 protein. The replacement of the Rac1 C-terminal polybasic domain with the C-terminal domain of Rac2 showed a reconstitution of ROS formation. Instead, the replacement of the Rac2 C-terminal domain with the Rac1 C-terminal polybasic domain did not (86). Thus, Rac2 is the key to the mediation of oxidase activation in neutrophils and downstream of chemoattractant (84).

In addition to neutrophils, Rac2 protein has been shown to be involved in T-cell development, a function shared with Rac1. Mice lacking Rac1 and Rac2 were detected to have a decreased number of mature CD4<sup>+</sup> T-cells, compared to mice lacking Rac1 only, or Rac2 only, which did not show to perturb T-cell development (82). Moreover, in Rac deficient mice, abnormalities in B-cell development have been also observed (82).

Human disease caused by dysfunction of the Rac2 protein have been described, showing combined clinical features of leukocytes adhesion deficiency (LAD) and CGD. The two patients reported presented defects in neutrophil adhesion and migration, along with neutrophilia and leukocytosis plus dramatic absence of pus in the infected areas. First, suspicion for LAD was ruled out when expression of CD11b/CD18 (commonly affected in LAD) was demonstrated. Further characterization of the neutrophils in these patients showed deficiency in activation of NADPH oxidase, which mirrors CGD. Missense



mutation was found on 169bp G>A (D57N), which results in a change of amino acid sequence (aspartate for asparagine). This mutation corresponds to the GTP binding pocket, that results in inactivation of not only Rac2 protein, but also Rac1 protein as well as other Rho GTPases (Figure 5) (82). Rac2 KO mice also show clinical features of LAD and CGD, however some overlapping functions are compensated by the expression of Rac1, as Rac2 KO mice preserve the GTP-binding pocket required for Rac1 to be active, compared to the human mutation. Thus, compared with the human scenario, Rac2 KO mice show normal T-cell development and lack of anemia.

The existence of Rac2 KO mice allowed for the *in vivo* study of the role of Rac2 in tissue inflammation. Rac2 has been comprehensively studied in acute lung injury (ALI), a common clinical disorder involving respiratory failure caused by injury to alveolar, epithelial and endothelial barriers in the lung. It can cause an acute respiratory distress syndrome that is associated with high morbidity and mortality, and the current available therapies fail to improve outcomes. Neutrophil recruitment and activation are primarily involved in ALI pathogenesis, leading to tissue-damage by degranulation and ROS release. Arthus reaction (hypersensitivity type III) was induced by intratracheal injection of rabbit anti-ovalbumin IgG (which induces the immune complex response). Rac2 KO mice showed less cellular inflammation regarding neutrophil count in response to increasing doses of antibodies to ovalbumin. The levels of cytokine release between wild-type mice and Rac2 KO mice were also examined. Cytokines' profiles did not show any significant difference between Rac2 KO and wild-type, however levels of myeloperoxidase (MPO; granule-derived mediator) which were significantly diminished in the Rac2 KO mice (87).

Another group also investigated the role of Rac proteins in ALI, but instead of using Rac2 KO mice, they pharmacologically inhibited Rac proteins with the molecule NSC23766 and compared its efficacy with dexamethasone (glucocorticoid). NSC23766 is a Rac-specific small-molecule inhibitor that inhibits Rac binding and activation through Rac-specific GEF, thus inhibiting both Rac1 and Rac2. Yao et al. studied the ALI induced by lipopolysaccharide (LPS, a component of gram-negative bacteria cell wall), which not only

triggers neutrophil infiltration but also induces neutrophil release of pro-inflammatory mediators, such as tumor necrosis factor- $\alpha$ , IL-1 $\beta$ . NSC23766 was injected to wild-type mice using two different doses, one group at 1 mg/kg, and another group at 3 mg/kg. Both groups showed a reduced number of total inflammatory cells and neutrophils as compared with non-treated mice (positive control group). However, the reduced number of inflammatory cells observed in Dexamethasone group was only similar to the group receiving NSC23766 at 3 mg/kg, showing a dose-dependent efficacy of NSC23766. MPO activity was also compared, achieving similar results at higher doses of NSC23766 to those treated with dexamethasone at 1 mg/kg (88). Therefore, NSC23766 shows an anti-inflammatory effect that is similar to those exerted by dexamethasone at high doses. Even though ALI and EBA have different pathogenesis, neutrophils and NADPH oxidase seems to participate similarly in tissue injury development. Following the hypothesis studied in ALI, we decided to investigate the role of the Rac2 protein in tissue injury in the passive transfer EBA animal model.



## **4. OBJECTIVES**

---



#### **4. OBJECTIVES**

The primary objective of this project was to investigate the *in vivo* the role of the innate immune system, specifically the role of neutrophils, in experimental EBA. As stated above, the presence of neutrophils may induce ROS formation leading to BMZ disruption and subsequent blister formation. We hypothesize that the absence of Rac2 protein (which mainly participates in neutrophil recruitment and ROS release by these leukocytes) may protect mice from disease development induced by the passive transfer of pathogenic anti-CVII antibodies.

The secondary objective of this study was to assess the efficacy of the pharmacological inhibition of Rac2 protein (NSC23766) in passively induced EBA in wild-type mice. Avoiding disease development by using an inhibitor would potentially establish a new therapeutic weapon. At the same time and assuming benefit of Rac2 protein inhibition, we aim to compare it with the effect of current therapies known to benefit EBA patients, such as dexamethasone and dapsons.



## **5 . MATERIALS AND METHODS**

---





## 5. MATERIALS AND METHODS

### *5.a Mice*

Six to 8-week-old C57BL6/J female mice with a bodyweight of ~17 g were obtained from Charles River Laboratories (Wilmington, MA, USA). Breeding pairs of Rac2 KO mice with C57BL6/J background were obtained from Boston Children's Cancer Center and Blood Disorders Center. KO mice were also mixed with WT mice. Inbred mice were genotyped. Only those homozygous for either Rac2 KO or WT were used in each experiment. All injections and blood draws were performed on mice anesthetized by inhalation of isoflurane. The experiments were approved by local authorities of the Animal Care and Use Committee (JHG-10-1250P2) and performed by certified personnel. Wild-type mouse strains were reported to be susceptible for the induction of skin blistering by the passive transfer of CVII-antibodies (43).

### *5.b. Mice genotyping*

Genotyping of the mice was performed as follows. Samples of tails were taken from all mice and DNA extracted for genotyping by PCR. All the primers for PCR genotyping were used at 0.5 mM final concentration. With 8 µl of APEX Taq Red Master Mix 2.0X primers used were: 1 µl for exon 1: CAC ACA CTT GAT GGC CTG CAT, 1 µl for control: GAC GCA TGC TCC ACC CCC T; and 1 µl pGKneo plasmid: TGC CAA GTT CTA ATT CCA TCA GAA GC. PCR buffer (10x): 750 mM Tris-HCl (pH 9.0), 500 mM KCl, 200 mM (NH<sub>4</sub>)<sub>2</sub>SO<sub>4</sub> and 2 mM dNTPs. An aliquot of 0.6 U Biotools DNA polymerase (Biotools B&M Labs, SA, Madrid, Spain) was used per sample. Thermocycling: initial step was set at 94°C for 5 min, followed by 35 cycles of 30 seconds at 94 °C, 1 min at 62 °C, and 1 min 72 °C, followed by 7 min at 72 °C. The DNA bands were separated in a 1% agarose gel. Size identifying WT mice was 245bp and for KO mice was 170 bp.

### *5.c. Recombinant protein CVII*

The recombinant form of murine CVII corresponding to fragment Cr (referred below as mCVIICr) (aa 759-980) was expressed as glutathione-S-transferase (GST) fusion protein in *Escherichia coli* as previously described (89). The full-length form of murine collagen VII was obtained following published protocols (47, 90). Briefly, the cDNA sequence coding specifically for the fragment of the NC1 was cloned into pcDNA5/FRT vector and expressed in Flp-In HEK 293T human embryonic kidney cells (Flp-InTM- 293; Invitrogen, Carlsbad, CA, USA). The construction of the entire cDNA sequence utilized the overlapping internal restriction sites including NheI, Asp, AgeI, AvrII and AarI from each cDNA fragment. DNA sequence data for murine collagen VII was retrieved from GenBank using the accession number NM\_007738 [http://www.ncbi.nlm.nih.gov/gene/?term=NM\\_007738](http://www.ncbi.nlm.nih.gov/gene/?term=NM_007738). Seventy per cent confluent Flp-In HEK 293T human embryonic kidney cells were transfected with 3 µg of recombinant vector. When they reached 90% confluence, they were grown in serum-free DMEM medium, without phenol red (Gibco, Darmstadt, Germany) supplemented with L-glutamine, penicillin, streptomycin, hygromycin (all from Biochrome, Berlin, Germany) and 100 µg/ml vitamin C. Two days after medium change and vitamin C addition, the medium was collected, centrifuged, PMSF and EDTA were added to a final concentration of 0.1 and 0.5 M respectively, and stored at 20°C. The recombinant murine CVII fragment was concentrated from the harvested culture media by 30% ammonium sulfate precipitation.

### *5.d. Rabbit immunization*

Four New Zealand White rabbits (Eurogentec, Seraing, Belgium) were immunized subcutaneously with 200 mg of purified, recombinant protein in Freund's complete adjuvant. The animals received two boosting injections with the same protein amount suspended in incomplete Freund's adjuvant at 2 week-intervals. Immune sera were obtained at regular intervals and tested by immunofluorescence microscopy on

cryosections of murine skin. Unspecific rabbit IgG was obtained from C.C.pro (GmbH, Neustadt, Deutschland).

#### *5.e. Affinity purification of IgG*

Total IgG from immune and normal rabbit serum was isolated using Protein G Sepharose 4 Fast Flow affinity column chromatography (GE Healthcare, Freiburg, Germany). Antibodies were eluted with 0.1 M glycine buffer (pH 2.5), neutralized with 1.5 M Tris-HCl (pH 10), and concentrated under extensive washing with PBS (pH 7.2) using Amicon Ultra-15 filters (Millipore, Darmstadt, Germany). The concentration of the purified IgG was measured spectrophotometrically at 280 nm (Nanodrop 1000 Spectrophotometer, Thermo Fisher Scientific, Waltham, Massachusetts).

#### *5.f. Induction of experimental EBA*

Experimental EBA was induced by passive transfer of rabbit anti-mCVIIc IgG in WT and Rac2 KO mice, as described with minor modifications (43). A total of 60 mg of purified rabbit anti-mCVIIc IgG was injected to each mouse, equivalent to the purified unspecific rabbit IgG dose injected to negative controls. Mice were bled before the first immunization and every other day thereafter for a period of 12 days. Mice were weighed and evaluated every second day for clinical signs of EBA, such as erythema, blisters, scarring, erosions, crusting and alopecia. The extent of the disease activity was determined by quantifying the affected skin surface area (see scoring system in Table 7). Because blood was drawn from tail before each antibody injection, tail was not considered in the clinical assessments. Biopsies of lesional and perilesional skin were collected after the euthanasia of mice, and subsequently prepared for immunofluorescence microscopy and histopathology. Intact blisters, erosions crusts and alopecia were quantified and the extent of skin disease was scored as follows: 0, no lesions; 1, less than 1% of the skin surface; 2, 1–5% of the skin surface; 3, 5–10% of the

skin surface; 4, 10–20% of the skin surface; 5, greater than 20% of skin surface affected. In our project, in order to avoid misdiagnosis between trauma induced and disease development, tail was not included in the assessment as this was the location of the blood draw.

**Table 7.** Clinical score depending on the body surface area (BSA) involved.

| Clinical score | BSA involved            |
|----------------|-------------------------|
| 0              | 0%, no lesions detected |
| 1              | <1%                     |
| 2              | 1 – 5%                  |
| 3              | 5 – 10%                 |
| 4              | 10 – 20%                |
| 5              | >20                     |

#### *5.g. Drugs administration*

NSC23766, (N6-[2-[(4-(Diethylamino)-1-methylbutyl)amino]-6-methyl-4-pyrimidinyl]-2-methyl-4,6-quinolinediamine trihydrochloride), and dexamethasone (DEX) were purchased from Tocris Bioscience (Bristol,UK). Dapsone (4,4'-Diaminodiphenyl sulfone) was purchased on Sigma-Aldrich (St Louis, MO, USA). NSC23766 was administered intraperitoneally at 7 mg/kg, Dexamethasone was administered subcutaneously at 1 mg/kg (88, 91, 92), and Dapsone was administered orally with a feeding needle (18-20 gauge) at 2 mg/kg (93). Mice were pre-treated with daily doses of each drug during one week prior and afterwards to the passive transfer of rabbit anti-mCVIICr IgG and unspecific rabbit IgG.

#### *5.h. Histology*

Biopsies of lesional skin were fixed in 3.7% buffered formalin. Sections from paraffin-embedded tissues were stained by haematoxylin and eosin.

### *5.i. Immunofluorescence microscopy*

Serum and tissue bound rabbit or mouse antibodies were detected following published protocols with minor modifications (43). Briefly, after incubating with serial dilutions of rabbit immune sera or affinity-purified total rabbit IgG, the frozen sections of normal and/or salt-split murine skin were treated with 100-fold diluted, FITC- conjugated Abs to rabbit IgG (Sigma-Aldrich; St Louis, MO, USA). Direct IF microscopy was performed on frozen sections, obtained from murine tissue biopsies, using 50-fold diluted FITC-conjugated Abs to rabbit IgG (Sigma-Aldrich; St Louis, MO, USA), and murine C3 (MP Biomedicals Cappel, Solon, OH, USA), respectively. Slides were observed with the fluorescence microscope (Olympus BX51, Olympus, San Diego, CA).

### *5.j. ELISA*

To measure the serum levels of rabbit antibodies against CVII, ELISA was performed as described, with minor modifications (52). Briefly, each well of the polystyrene plates (Maxisorb Immunoplate, Nunc, Germany) was coated overnight with 200 ng of recombinant protein mCVIICr in 0.1 M bicarbonate buffer (pH 9.6). After blocking, wells were incubated with a 100- fold dilution of mouse sera for 60 min. Bound Abs were detected using a 10,000-fold horseradish peroxidase (HRP)-conjugated anti-rabbit IgG (Sigma-Aldrich; St Louis, MO, USA), and secondary antibody union was detected by chemiluminescence, by adding 3,3',5,5'-tetramethylbenzidine (DAB) (Sigma-Aldrich, St Louis, MO, United States). The reaction was stopped by adding 1M H<sub>2</sub>SO<sub>4</sub> (50 µl/well), afterwards optical densities (OD) were read at 450 nm using a microplate reader (Tecan Infinite® 200; Tecan Group Ltd, Maennedorf, Switzerland).

#### *5.h. Statistical analysis*

Descriptive statistics including median (with range) and counts (with percentages) were determined and compared using U Mann Whitney (two groups) or Kruskal-Wallis (for multiple groups) and Fisher's Exact tests, respectively. All tests were performed using SPSS statistics software (Chicago, IL, USA) with a type I error rate of 5%. P-values less than 0.05 were considered indicative of a trend.

## **6. RESULTS**

---





## 6. RESULTS

### ***6.a. Rabbits immunized with mCVIIcCr produced high titers of IgG antibodies that recognize mouse BMZ.***

IIF was performed with rabbit sera against murine skin to assess the presence of antibodies with affinity to the BMZ. Median titer of post-immunized rabbit sera was 1:20,000, with the highest titer detected at 1:40,000. IIF on salt-split murine skin showed deposition on the dermal side of the blister (Figure 6).

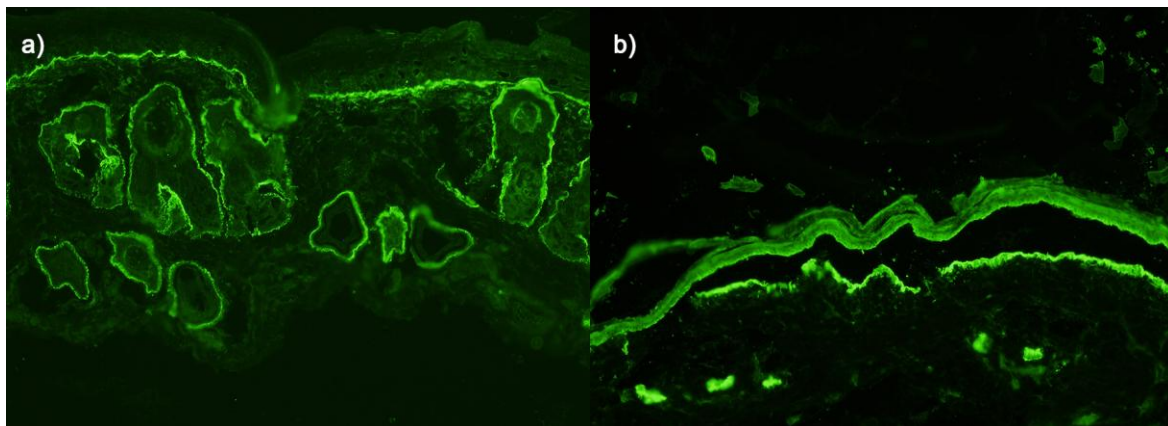


**Figure 6. Sera from immunized rabbit with mCVIIcCr showed IgG deposition at the murine BMZ by IIF. a) IIF (x10) at 1:5000 dilutions of rabbit sera with anti-CVII IgG against murine skin. Linear deposition of rabbit IgG against mCVIIcCr is seen along the BMZ of epidermis and follicles. b) IIF (x10) at dilution of 1:100 of rabbit sera with anti-CVIIcCr IgG on salt-split of murine skin. Linear deposition of rabbit IgG is seen on the dermal side of the epidermis.**

***6.b. Passive transfer of rabbit anti-mCVIIICr IgG in wild-type mice induced EBA phenotype.***

Rabbit anti-mCVIIICr IgG was tested in a pilot study. Group 1 (G1) including three WT C57BL6/J mice were injected with 45 mg of rabbit anti-mCVIIICr IgG (7.5 mg per day), and group 2 (G2) including three WT C57BL6/J mice were injected with 90 mg (15 mg per day) of the same preparation. A third group was injected with unspecific rabbit IgG as a negative control group.

***6.b.i. EBA phenotype***

Lesions started to appear at the 3<sup>rd</sup> dose in both groups. Alopecia associated with erythema was the most common type of lesion observed. Crusted patches and occasionally serohemorrhagic crusts were developed afterwards. These were mainly distributed on ears, eyes, upper and lower extremities, snout, neck and trunk. Disease severity was different between both groups due to the amount of antibody received. No skin lesions were observed on the negative control group.

***6.b.ii. Clinical differences between G1 and G2 based on BSA involved (Figure 7 – 9)***

At 3<sup>rd</sup> dose the median percentage of BSA was 1.16% (ranging from 0.49 to 2.47) for G1 and 3.02% (ranging from 1.1 to 5.05) for G2. Differences were not statistically significant ( $p=.27$ ) at this point. Instead, at the end of the experiment, median percentage of BSA affected for G1 was 11.69% (ranging from 8.4 to 12.07) and the median percentage of BSA involved for G2 was 18.03% (ranging from 14.53 to 23.12). Median percentage of BSA of G1 was significantly lower than G2 at 6<sup>th</sup> dose and at the end of experiment (both with a  $p=.05$ ).

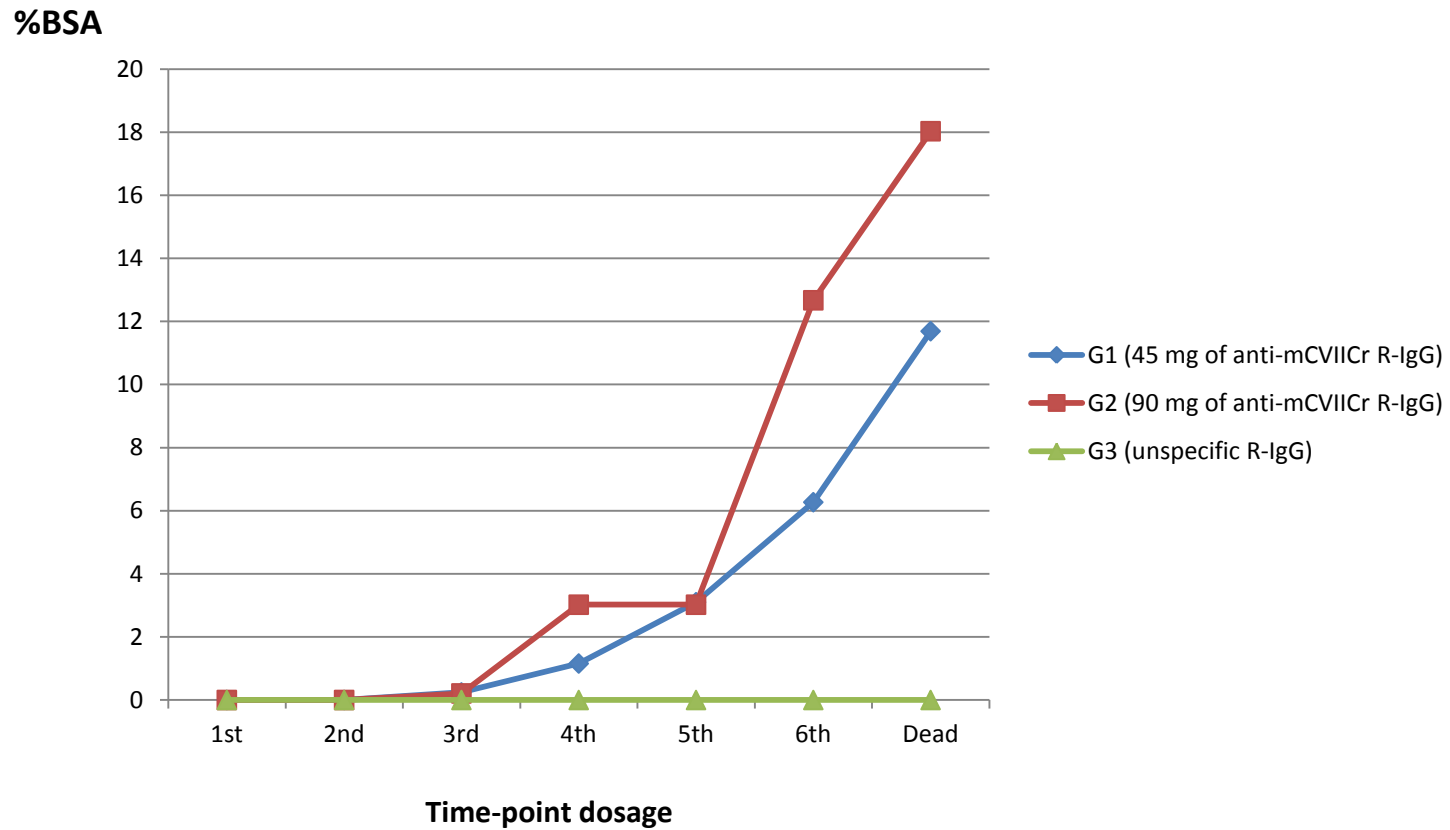


**Figure 7. Percentage of BSA involved in the three groups throughout disease development.** The increase of the median percentage of body surface area for each group of mice is represented. Y-axis is % of body surface area, x-axis represents de number of consecutive doses until the end of experiment. BSA: body surface area in percentage.

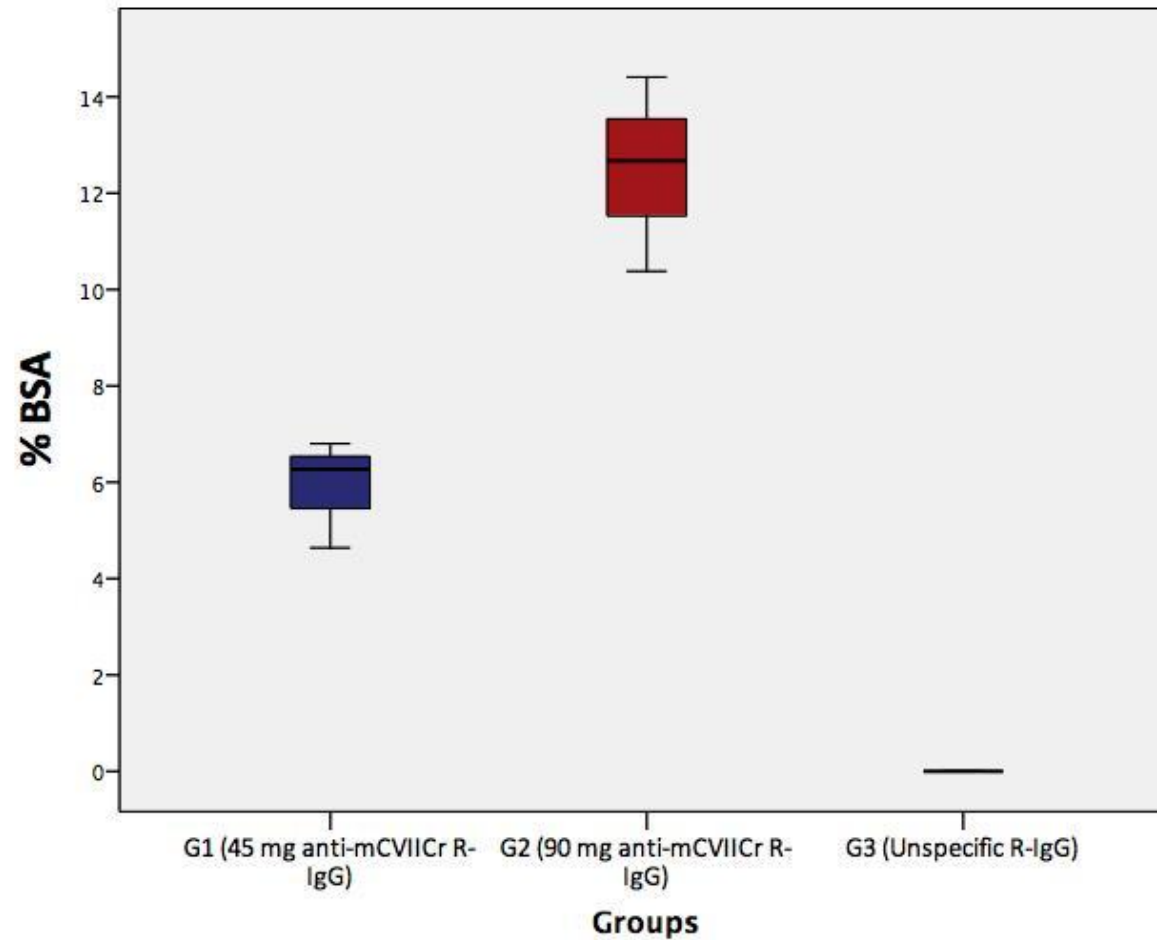


**Figure 8. Comparison of BSA involvement between groups showed a significant disease severity in G2 than in G1.** Median of BSA at dose 6<sup>th</sup> was significantly higher in G2 (18.03%; ranging from 14.53 to 23.12) compared with G1 (11.69%; ranging from 8.4 to 12.07) ( $p=.05$ ). Wild-type mice receiving unspecific R-IgG did not develop any type of lesion.

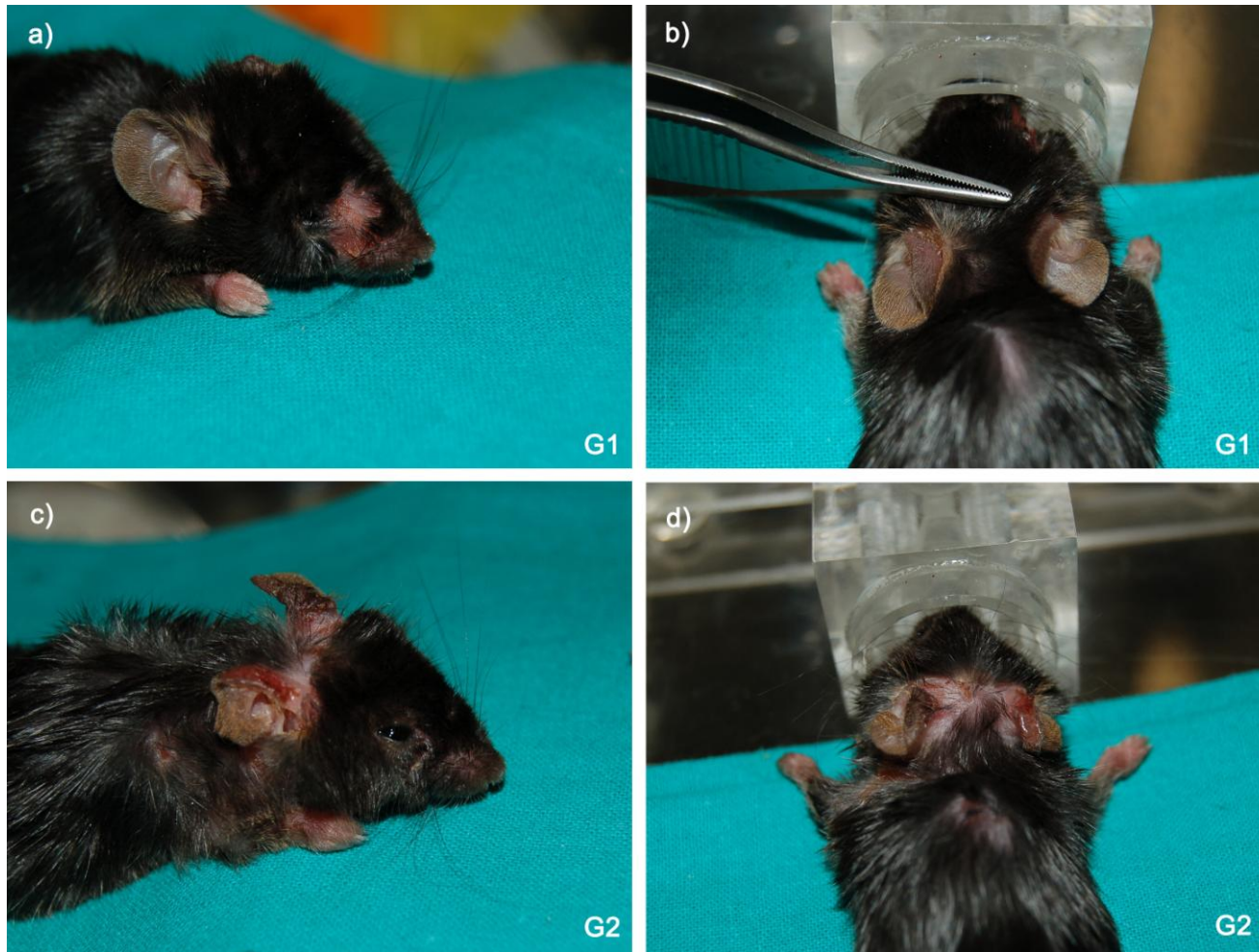


**Figure 9. Mice injected with IgG against mCVIIcR showed crusted plaques, alopecia and erosions.** a) Mouse injected with 45 mg of anti-mCVIIcR R-IgG, showing alopecia and erosions around the right eye and the right front leg. b) Mouse injected with 45 mg of anti-mCVIIcR R-IgG, showing left ear with scaly erythema. c and d) mice injected with 90 mg of anti-mCVIIcR R-IgG, showing extensive alopecia, erosion and right ear thickening. As observed in the pictures greater disease severity is seen in the second group. Clinical pictures shown correspond to 6<sup>th</sup> dose.

6.b.iii. Clinical differences between G1 and G2 based on clinical score

Comparison of clinical score between both groups resulted in a significantly higher score in G2 by the 6<sup>th</sup> dose (p=.03) (Table 8).

**Table 8.** Clinical score for each mouse throughout the experiment.

|                | 1 <sup>st</sup><br>Dose | 2 <sup>nd</sup><br>Dose | 3 <sup>rd</sup><br>Dose | 4 <sup>th</sup><br>Dose | 5 <sup>th</sup><br>Dose | 6 <sup>th</sup><br>Dose | Dead |
|----------------|-------------------------|-------------------------|-------------------------|-------------------------|-------------------------|-------------------------|------|
| <b>G1 (NN)</b> | 0                       | 0                       | 1                       | 1                       | 2                       | 3                       | 4    |
| <b>G1 (1T)</b> | 0                       | 0                       | 1                       | 2                       | 2                       | 2                       | 3    |
| <b>G1 (2T)</b> | 0                       | 0                       | 1                       | 2                       | 2                       | 3                       | 4    |
| <b>G2 (NN)</b> | 0                       | 0                       | 1                       | 3                       | 4                       | 4                       | 5    |
| <b>G2 (1T)</b> | 0                       | 0                       | 1                       | 2                       | 3                       | 4                       | 4    |
| <b>G2 (2T)</b> | 0                       | 0                       | 1                       | 2                       | 2                       | 4                       | 4    |
| <b>G3 (NN)</b> | 0                       | 0                       | 0                       | 0                       | 0                       | 0                       | 0    |
| <b>G3 (1T)</b> | 0                       | 0                       | 0                       | 0                       | 0                       | 0                       | 0    |

6.b.iv. Passive transfer of rabbit anti-mCVIIc IgG did not induced significant changes in weight between both groups receiving different amount of antibodies.

Weight loss was higher in G1 compared with G2, with no statistical significance (p=.09) (Table 9).

**Table 9.** Changes in weight for each mouse.

|                | Weight change throughout the<br>experiment (gr) |
|----------------|---|
| <b>G1 (NN)</b> | -2.2  |
| <b>G1 (1T)</b> | -1  |
| <b>G1 (2T)</b> | -0.4  |
| <b>G2 (NN)</b> | 1   |
| <b>G2 (1T)</b> | 0   |
| <b>G2 (2T)</b> | 1   |
| <b>G3 (NN)</b> | 2   |
| <b>G3 (1T)</b> | 2   |

*6.b.v. Injection of antibodies against mCVIIcR induces neutrophil-rich interstitial infiltrate and dermal-epidermal separation in skin biopsies of wild-type mice.*

Skin biopsies of lesional skin (involved ears) from G1 and G2 showed moderate to severe granulocyte infiltrate, ranging from moderate to severe, distributed from BMZ to deep dermis, (Figure 10 a – b). Dermal-epidermal separation was a common finding sometimes full-filled with neutrophils and forming intraepidermal neutrophil-abscesses (Figure 10 c – d). Serohemorrhagic crusts were seen in severe cases (Figure 10e). No cartilage involvement was seen in any of the specimens. Skin biopsies of G3 showed no neutrophilic infiltrate or dermal-epidermal separation.



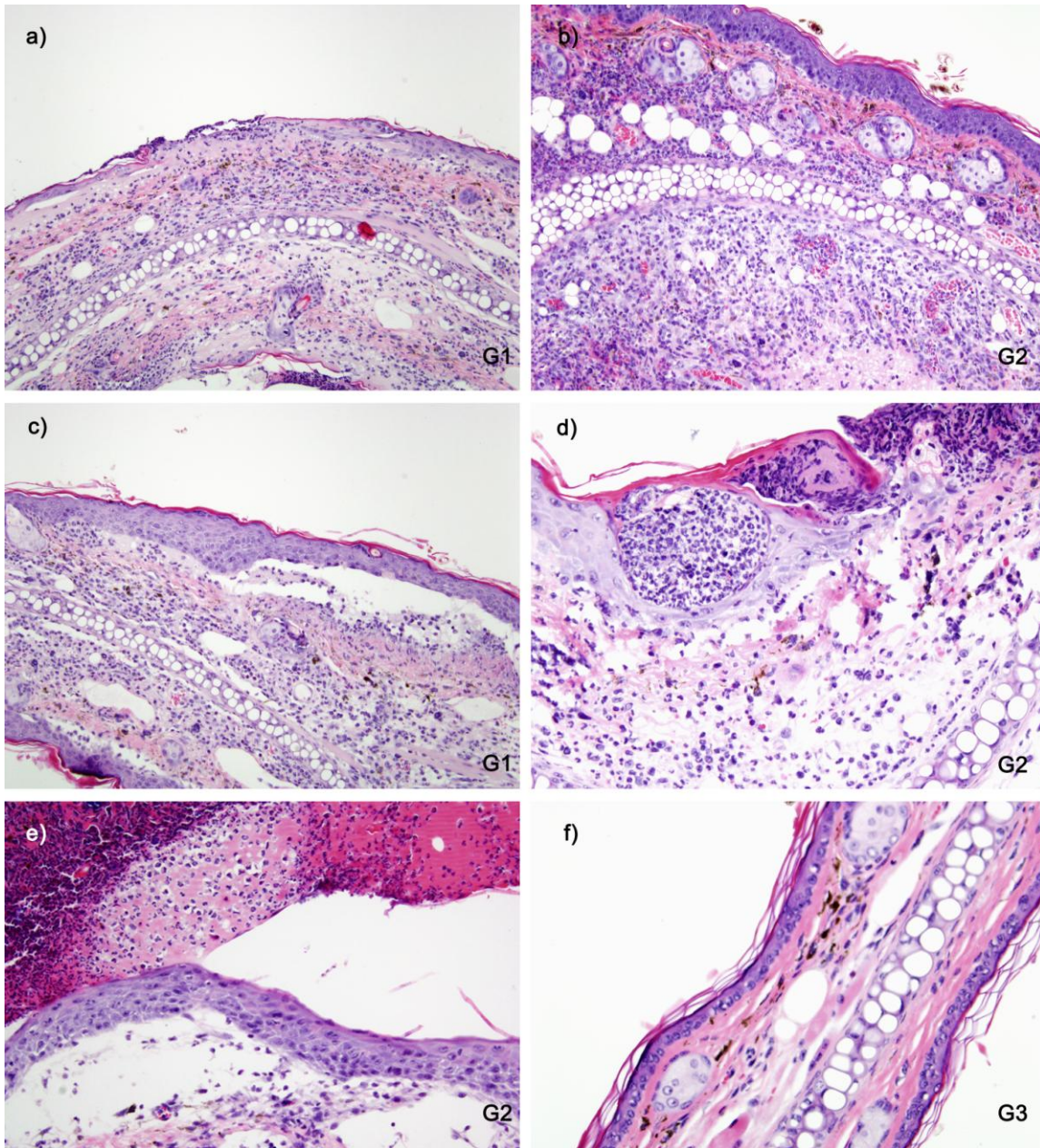


**Figure 10. Skin biopsies of mice receiving IgG against mCVIIc<sub>r</sub> showed neutrophil-rich infiltrate and dermal epidermal separation. G1 (a,c), G2 (b,d), G3 (f). a) Moderate granulocyte infiltrate at the dermis extending almost to cartilage, HE x10. b) Severe dermal infiltrate with thickening of the dermis, HE x20. c) Dermal epidermal separation, with neutrophils filling the bulla HE x10. d) Neutrophil abscess on the epidermis associated with a thick crust at the stratum corneum HE x40. e) Dermal-epidermal separation with serohemorrhagic crust formation HE x40. f) Normal skin biopsy of the mice ear, without dermal infiltrate or dermal-epidermal separation, and normal ear thickening.**

6.b.vii. Rabbit anti-mCVIIc IgG and murine C3 were detected at the BMZ on the perilesional skin of wild type mice with skin lesions.

Linear deposition of rabbit IgG was seen along the BMZ of the epidermis and hair follicles in all skin biopsies of both groups G1 and G2 (Figure 11 a-b). Deposition of murine C3 was detected on BMZ and also around hair follicles of both groups receiving rabbit anti-mCVIIc IgG (Figure 11 c-d). G3 receiving unspecific rabbit IgG did not show any deposition at the BMZ.

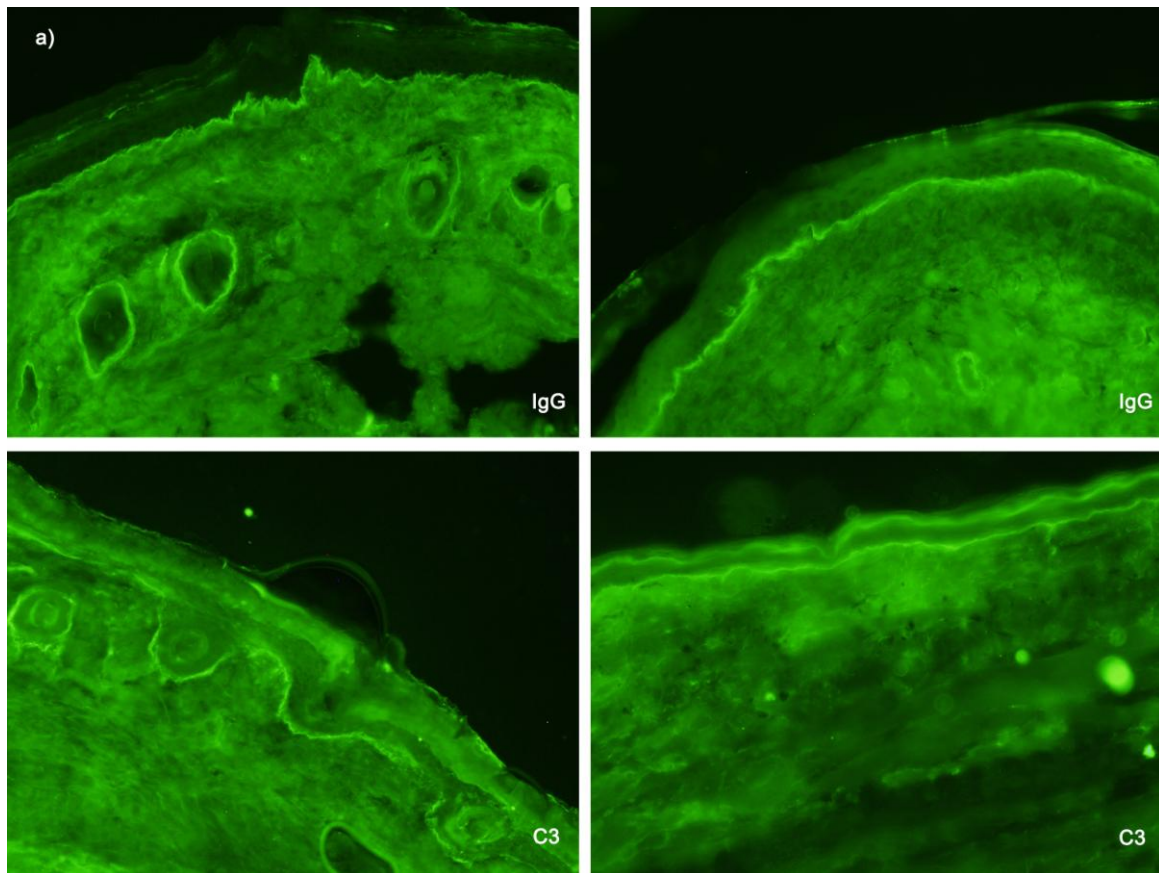


**Figure 11. DIF of perilesional skin of mice receiving rabbit anti-mCVIIc IgG showed both, deposition of rabbit IgG and murine C3 at the BMZ of the epidermis and hair follicles. a) Linear deposition of IgG at the BMZ of hair follicles, DIF IgG x20. b) Linear deposition of IgG at the BMZ, DIF IgG x40. c) Linear deposition of C3 at the BMZ of the epidermis and hair follicles, DIF C3 x20. d) Linear deposition of C3 at the BMZ, DIF C3 x40.**

6.b.viii. Rabbit antibodies against mCVIIcR are detected in blood of wild-type mice with EBA phenotype

Mice' sera from all three groups were analyzed by ELISA for total circulating levels of IgG against mCVIIcR from before IgG was injected through days receiving 4<sup>th</sup> and 6<sup>th</sup> doses. Increased levels of IgG were seen in both groups throughout all the experiment receiving rabbit anti-mCVIIcR IgG. No statistical differences were detected between both groups ( $p=0.27$ ), G1 and G2 (Figure 12).

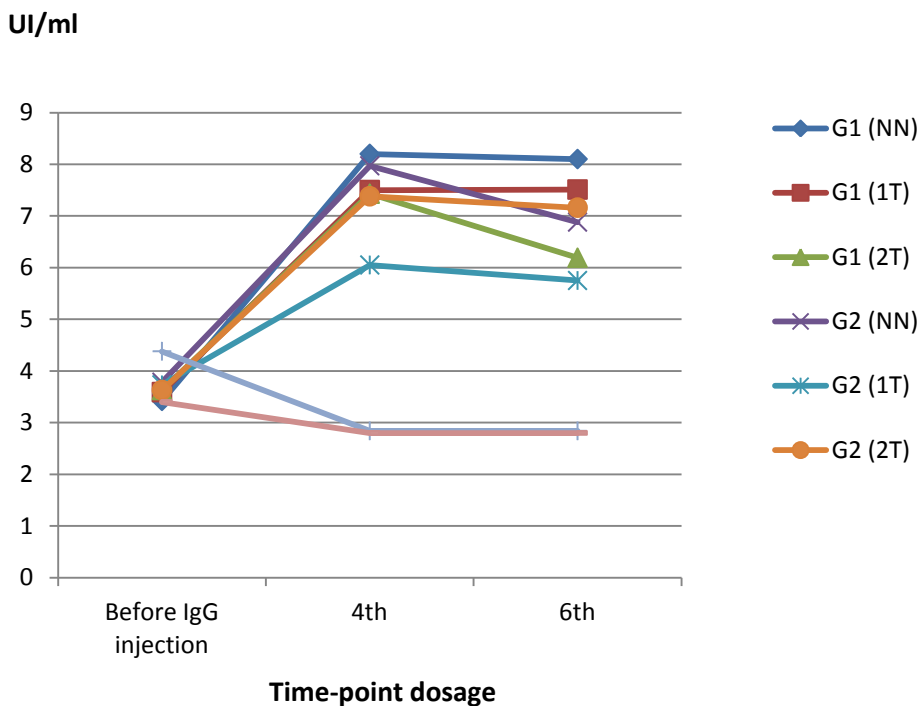


**Figure 12. Total serum levels of rabbit anti-mCVIIcR IgG for each group throughout the experiment.** Sera from WT mouse injected with rabbit anti-mCVIIcR IgG showed increased levels of circulating antibodies.

Based on these results, further sets of experiments were performed at a total dose of 60 mg (10 mg/day) of IgG (rabbit anti-mCVIIcR and unspecific rabbit IgG).

**6.c. Rac2 KO mice injected with rabbit anti-mCVIIc IgG did not developed blisters, erythema, or serohemorrhagic crusts suggestive of EBA phenotype.**

Two sets of Rac2 KO mice (first group) n=5; second group n=5) were injected with rabbit anti-mCVIIc IgG. Both sets were injected with 60 mg (10 mg per dose) and 50 mg (10 mg per dose) of rabbit anti-mCVIIc IgG, respectively. Two sets of 4 Rac2 KO mice were each injected with unspecific rabbit IgG as negative controls, in addition to three WT mice that were used as positive controls.

**6.c.i. EBA phenotype**

None of the Rac2 KO mice receiving rabbit anti-mCVIIc IgG showed blister, erosions or alopecia formation after 5 or 6 doses of antibodies (Figure 13). Positive control group showed erythematous alopecic patches on ears, around eyes, snout, upper and lower extremities starting on the 3<sup>rd</sup> dose of rabbit anti-mCVIIc IgG. Median percentage of BSA at this point was 1.79 (ranging from 0.2 – 2.42) (clinical score=2). Median percentage of BSA at the end of the experiment was 12.35% (9.09 – 14.46) (clinical score=4) (Table 9).

**Table 9.** Clinical score of each mice of the positive control

| <b>Mice</b>               | <b>1<sup>st</sup> Dose</b> | <b>2<sup>nd</sup> Dose</b> | <b>3<sup>rd</sup> Dose</b> | <b>4<sup>th</sup> Dose</b> | <b>5<sup>th</sup> Dose</b> | <b>Dead</b> |
|---------------------------|----------------------------|----------------------------|----------------------------|----------------------------|----------------------------|-------------|
| <b>Positive Control 1</b> | 0                          | 0                          | 1                          | 2                          | 2                          | 4           |
| <b>Positive Control 2</b> | 0                          | 0                          | 2                          | 2                          | 3                          | 4           |
| <b>Positive Control 3</b> | 0                          | 0                          | 2                          | 2                          | 3                          | 3           |



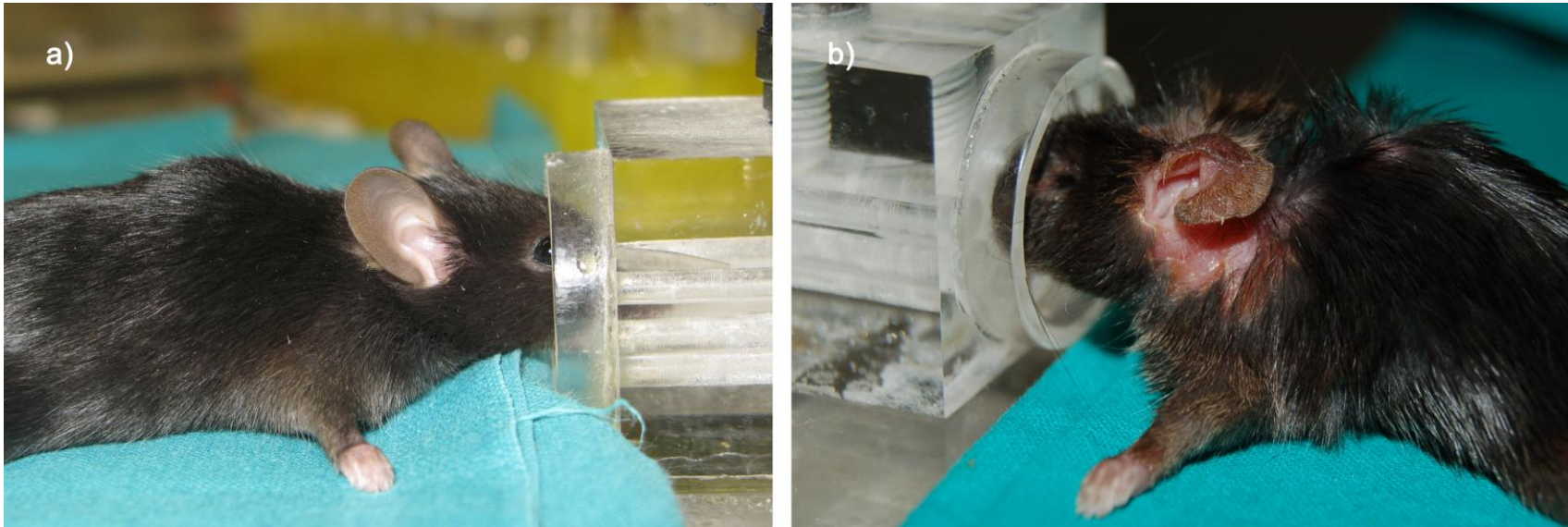


**Figure 13. Rac2 KO (a) mouse and WT mouse (b), both injected with rabbit anti-mCVIICr IgG.** a) Rac2 KO mouse showing completely healthy skin, with no blisters, erosions and crusted plaques at 6<sup>th</sup> dose. b) WT mice showing full-blown EBA phenotype manifested on the neck and ear.

6.c.ii. *Rac2* KO mice injected with rabbit anti-mCVIIcR IgG did not show significant weight loss compared with positive control group.

No significant weight loss was detected in any of the *Rac2* KO mice injected with rabbit anti-mCVIIcR IgG when compared with positive controls (p=.13) (Table 10).

**Table 10.** Weight changes for each mouse of all groups.

| Groups   | Mouse | Weight change throughout experiment (gr) |
|--|-------|--|
| <b>1<sup>st</sup> group of <i>Rac2</i> KO + anti-mCVIIcR R-IgG (n=5)</b> | 1     | 0  |
|  | 2     | 0  |
|  | 3     | 0  |
|  | 4     | -1                                       |
|  | 5     | -1                                       |
| <b>2<sup>nd</sup> group of <i>Rac2</i> KO + anti-mCVIIcR R-IgG (n=5)</b> | 6     | 2  |
|  | 7     | 0  |
|  | 8     | 0.5                                      |
|  | 9     | 1  |
|  | 10    | 2.1                                      |
| <b>1<sup>st</sup> group of <i>Rac2</i> KO + unspecific R-IgG (n=4)</b>   | 1     | 0  |
|  | 2     | 1  |
|  | 3     | 1  |
|  | 4     | -1                                       |
| <b>2<sup>nd</sup> group of <i>Rac2</i> KO + unspecific R-IgG (n=4)</b>   | 5     | 2.3                                      |
|  | 6     | -4.4                                     |
|  | 7     | 0.6                                      |
|  | 8     | 0.3                                      |
| <b>Positive control group (wild type mice) (n=3)</b>                     | 1     | 0.4                                      |
|  | 2     | -3.9                                     |
|  | 3     | -3.3                                     |

*6.c.iii. Skin biopsies of Rac2 KO mice injected with rabbit anti-CVIIc IgG did not show neither neutrophil-rich infiltrate nor dermal-epidermal separation.*

Skin biopsies (involved ears and trunk) of both groups of Rac2 KO mice receiving rabbit anti-mCVIIc IgG showed neither cellular infiltrate nor dermal-epidermal separation. Skin biopsies of mice receiving unspecific rabbit IgG did not show any infiltrate either. Skin biopsies of lesional skin of the positive control group showed the typical neutrophilic infiltrate along the dermis, and dermal-epidermal separation, similar to what was observed in the previous experiment (Figure 14).

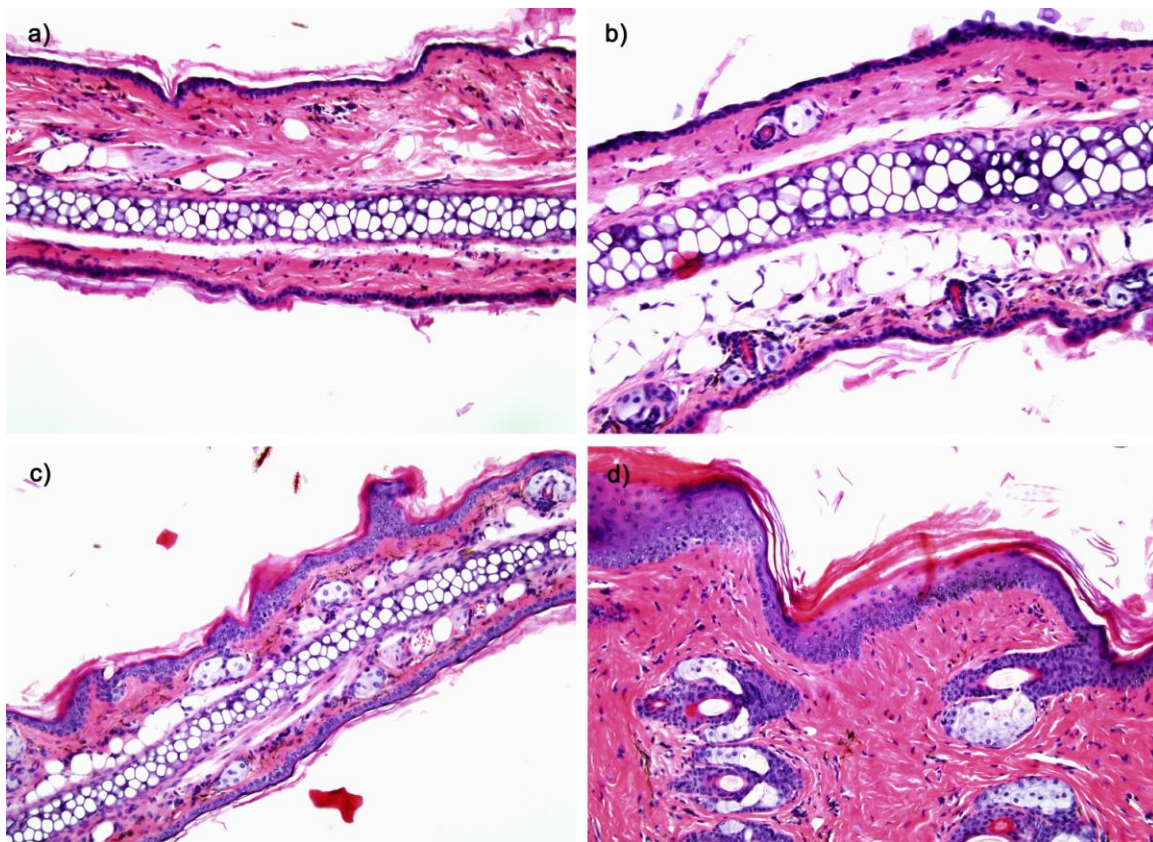


**Figure 14. Skin biopsies of Rac2 KO mice injected with rabbit anti-mCVIIc IgG showed neither infiltrate nor dermal-epidermal separation.** Murine skin biopsies of the ears (a,b,c) and trunk (d), without abnormalities, (a) HE x10, b) HE x20, c) HE x2, d) HE x40).

6.c.iv. Skin biopsies of Rac2 KO mice injected with rabbit anti-mCVIIICr IgG demonstrate deposition of rabbit IgG and murine C3 at the BMZ by DIF.

Murine skin biopsies from both groups of Rac2 KO mice injected with rabbit anti-mCVIIICr IgG showed linear deposition of rabbit IgG and murine C3 at the BMZ of the epidermis and hair follicle, as it was seen in the positive control group. Rac2 KO mice injected with unspecific rabbit IgG did not show any deposition at the BMZ (Figure 15).

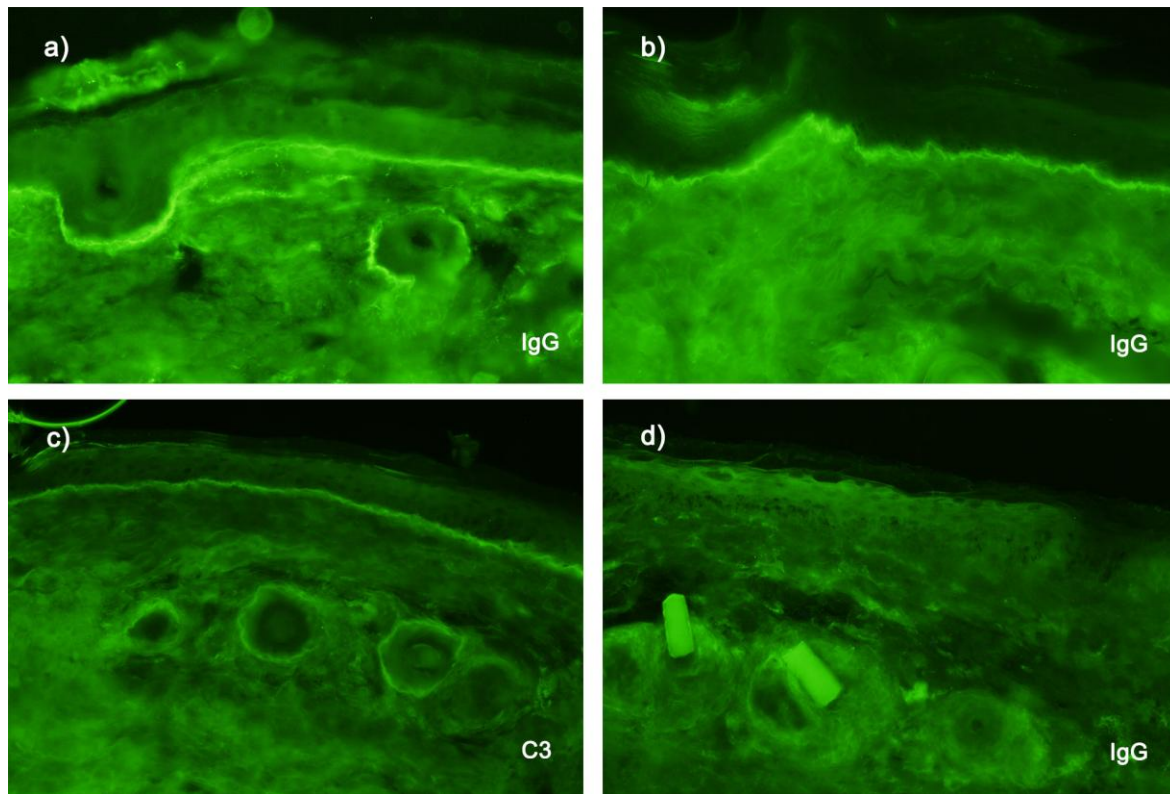


**Figure 15. Skin biopsies of Rac2 KO mice receiving rabbit anti-mCVIIICr IgG showed linear deposition of rabbit IgG and murine C3 by DIF.** Rabbit IgG (d,f) and mouse C3 (e) on skin biopsies from Rac2 KO mice. d) Linear deposition of IgG at the BMZ of epidermis and adnexa is seen (x20). e) Deposition of murine C3 is seen at the BMZ of the epidermis and adnexa. Image (f) shows a skin biopsy from a Rac2 KO mouse injected with normal rabbit IgG (negative control).



6.c.v. *Rac2* KO mice injected with rabbit anti-mCVIIcR IgG showed increased circulating IgG levels.

Increased levels of circulating rabbit anti-mCVIIcR IgG were detected in mice' sera by ELISA in both groups of *Rac2* KO mice injected with rabbit anti-mCVIIcR IgG, throughout the experiment (Figure 16 and 17). Negative controls did not show circulating levels of rabbit anti-mCVIIcR IgG in any of the two groups injected with unspecific rabbit IgG.

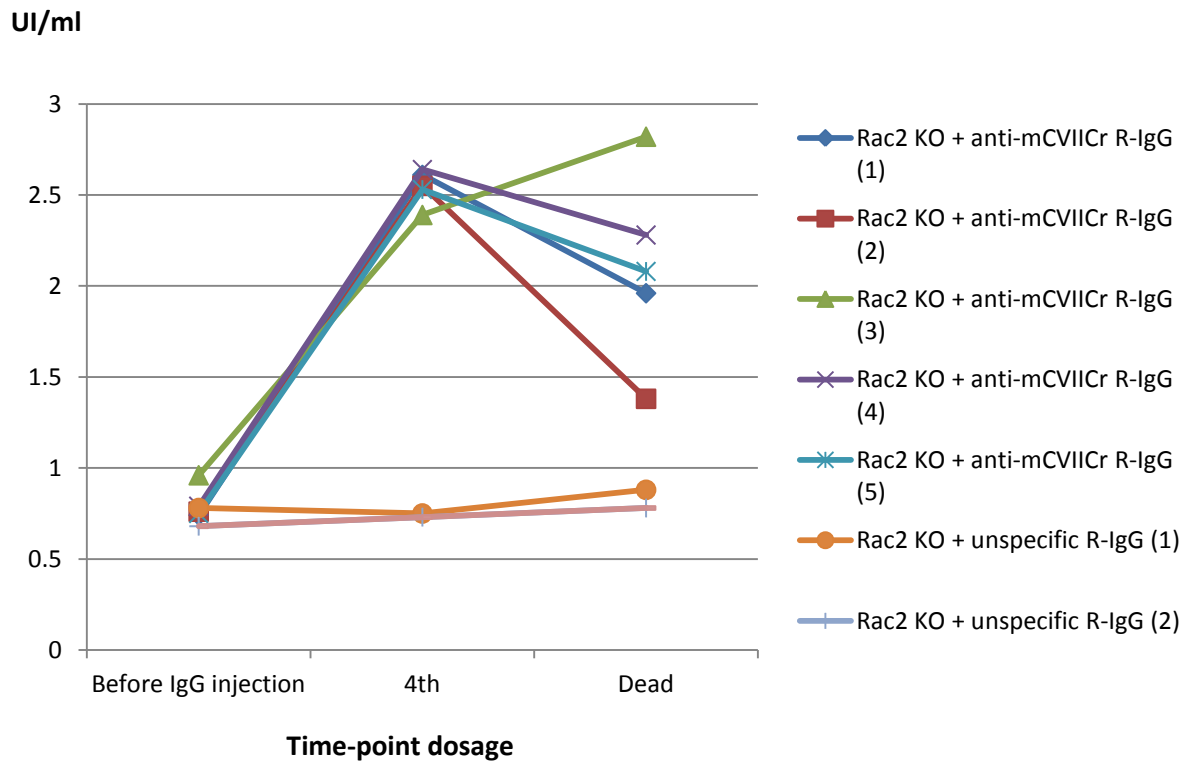


**Figure 16. ELISA results of the first group of *Rac2* KO mice (n=5). Total levels of rabbit anti-mCVIIcR IgG for each group throughout the experiment. Sera from *Rac2* KO mouse injected with rabbit anti-mCVIIcR IgG showed increased levels of circulating anti-mCVIIcR antibodies compared with the group that received unspecific rabbit IgG.**

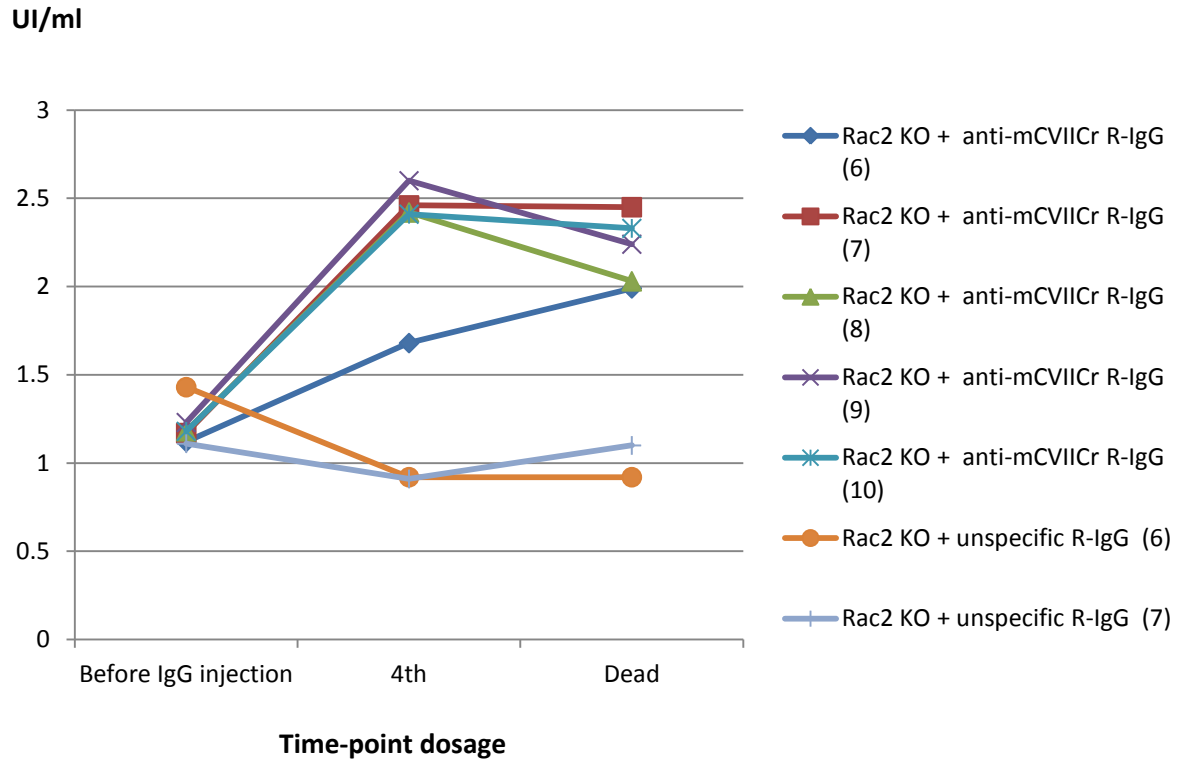


**Figure 17. ELISA results of the second group of Rac2 KO mice (n=5). Total levels of rabbit anti-mCVIICr IgG for each group throughout experiment.** Sera from Rac2 KO mouse injected with rabbit anti-mCVIICr IgG showed increased levels of circulating anti-mCVIICr antibodies compared with the group that received unspecific rabbit IgG.

A summary of the all the results obtained for the experiments performed in Rac2 KO mice are shown in table 11.

**Table 11.** Summary of clinical, histological, DIF and ELISA results obtained for both groups of Rac2 KO mice compared with wild type group.

| <b>Groups (number of mice per group)</b>                       | <b>Clinical score at death<br/>Median, range</b> | <b>Weight changes<br/>Median, range</b> | <b>DIF R-IgG</b> | <b>DIF murine C3</b> | <b>ELISA anti-mCVIIcR R-IgG</b> |
|--|--|---|------------------|----------------------|---------------------------------|
| <b>Rac2 KO 1<sup>st</sup> group + anti-mCVIIcR R-IgG (n=5)</b> | 0  | 0 (-1 - 0)                              | Linear at BMZ    | Linear at BMZ        | +                               |
| <b>Rac2 KO 2<sup>nd</sup> group + anti-mCVIIcR R-IgG (n=5)</b> | 0  | 1 (0.5 – 2.1)                           | Linear at BMZ    | Linear at BMZ        | +                               |
| <b>Rac2 KO 1<sup>st</sup> group + unspecific IgG (n=4)</b>     | 0  | 1 (0 - 2.1)                             | Negative         | Negative             | -                               |
| <b>Rac2 KO 2<sup>nd</sup> group + unspecific IgG (n=4)</b>     | 0  | 0.6 (-4.4 - 2.3)                        | Negative         | Negative             | -                               |
| <b>Positive control group (wild-type mice) (n=3)</b>           | 4 (3 – 4)  | -3.3 (-3.9-0.4)                         | Linear at BMZ    | Linear at BMZ        | +                               |

***6.d. Wild type mice pre-treated with NCS23766 developed blisters, erosions and alopecic patches after the injection of rabbit anti-mCVIIICr IgG.***

Three groups of wild type mice were pre-treated with NCS23766 (n=3), dexamethasone (n=3) and dapsonsone (n=5) before passive transfer of 10 mg of rabbit anti-mCVIIICr IgG. Positive control group (n=3) corresponded to wild-type mice receiving rabbit anti-mCVIIICr IgG without pre-treatment and the negative control group (n=2) corresponded to wild-type mice receiving unspecific rabbit IgG.

*6.d.i. EBA phenotype*

Alopecia and erythematous patches, as well as, scaly and crusted patches were seen in each group receiving rabbit anti-mCVIIICr IgG starting at 3<sup>rd</sup> dose, yet being more evident at 4<sup>th</sup> dose for the mice belonging to the pre-treated groups (Figure 18 – 19). At 6<sup>th</sup> dose all presented the same clinical score.

*6.d.ii. Disease severity was not significantly decreased in any of the pre-treated group when compared with the positive control group.*

BSA involvement at 6<sup>th</sup> dose was 5.64% (ranging from 5.06 – 11.31) (clinical score=3) in the group receiving dexamethasone, 6.42% (ranging from 3.79 – 9.58) (clinical score=3) in the group receiving dapsonsone, and 8.19% (ranging from 7.90 – 13.70) (clinical score=3) in the group receiving NCS23766, and 9.88% (clinical score=3) in non-pre-treated mice. Comparison of the median BSA involved performed at 6<sup>th</sup> dose did not show any statistical significance in pre-treated groups when compared with the positive control (non-pretreated group) (p=.27, p=.18 and p=.83, respectively). Even though, initially there was a trend of milder disease in the pre-treated groups (meaning that disease appeared to start later in the pre-treated group than in non-pre-treated group), at dose 6<sup>th</sup> significant differences in BSA involvement between groups could not be demonstrated (p=.08) (Figure 19 and 20).

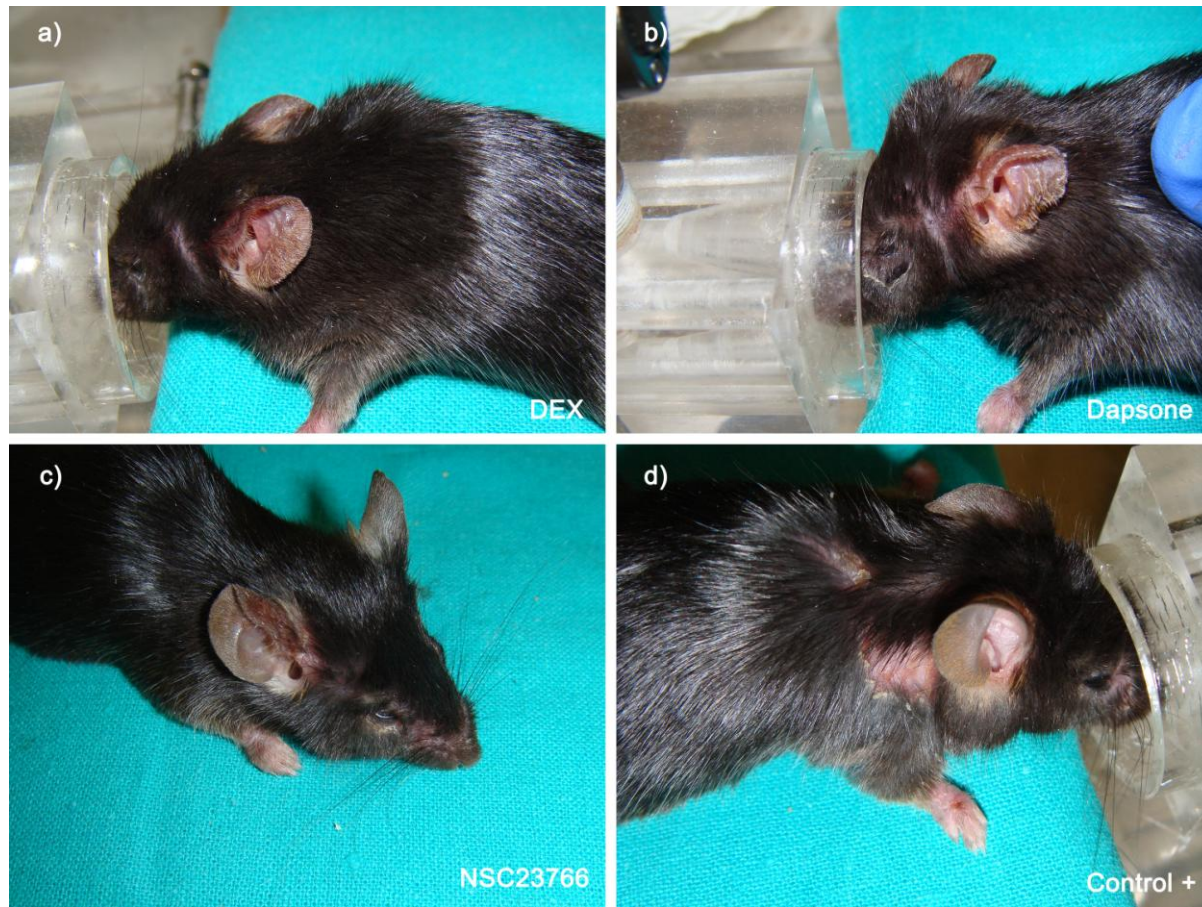


**Figure 18. WT mice pre-treated and positive control group (non-pretreated mice) are shown. a) Mouse pre-treated with dexamethasone showing ear thickening and erythema. b) Pre-treated mouse with dapsone showing ear thickening and mild scaling. c) Pre-treated mouse with NSC23766 showing ear thickening and mild alopecia on the right face. d) Non-pretreated mice showing extensive alopecia on the posterior trunk.**

## % BSA

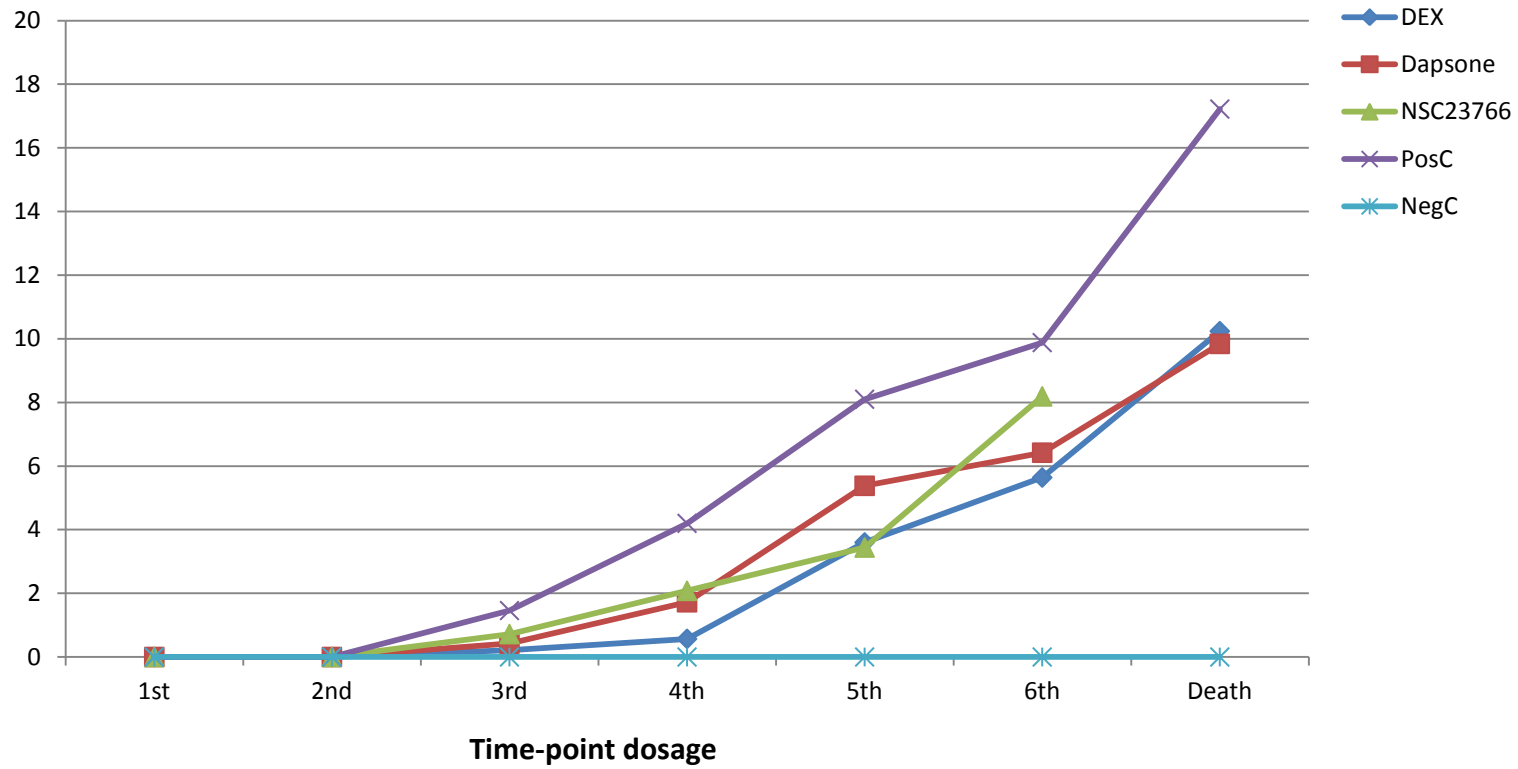


**Figure 19. Comparison of body surface area involved throughout disease development for each group.** The median of percentage of body surface area involved throughout disease showed a milder severity among pre-treated mice with dexamethasone (DEXA), dapson (DAP) or the Rac2 inhibitor NSC23766, compared with the positive control group. Y-axis is the % of body surface area, x-axis is the doses that each mouse received until the end of the experiment. DEX: dexamethasone; PosC: positive control; NegC: negative control

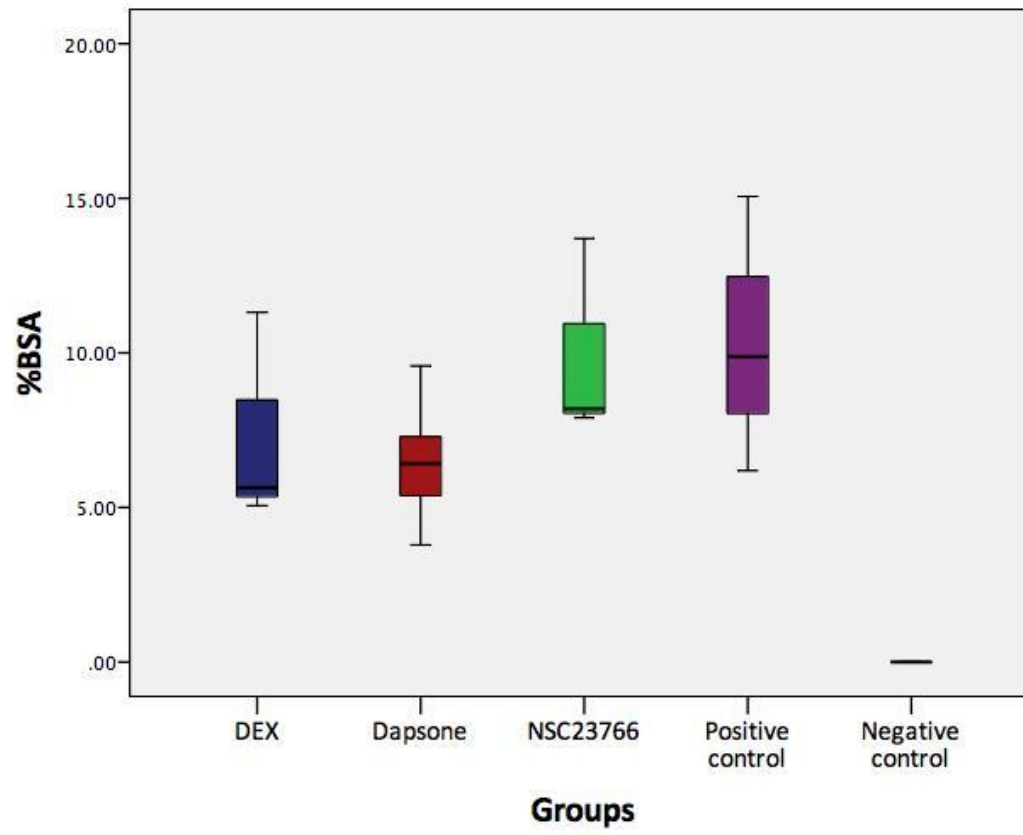


**Figure 20. Disease severity was not statistically significant among different groups at dose 6<sup>th</sup>.** Box plot showing the median and ranges of body surface area involved by disease for each group. The overlapping ranges show no statistical significant differences among all four groups.

6.d.iii. Weight loss was not significantly observed in the positive control group when compared with the pre-treated groups.

No significant weight loss was observed in positive control group when compared with each pre-treated groups; dexamethasone group ( $p=.18$ ), dapsone group ( $p=.45$ ), or NSC23766 group ( $p=.27$ ).

**Table 12.** Weight changes for each mouse of the pre-treated, positive control and negative control groups.

| Groups           | Mice | Weight changes (gr) |
|------------------|------|---------------------|
| Dexamethasone    | 1    | -1.2                |
|                  | 2    | -1.4                |
|                  | 3    | -1.4                |
| Dapsone          | 1    | 1.3                 |
|                  | 2    | -0.3                |
|                  | 3    | -1.7                |
|                  | 4    | -2.6                |
|                  | 5    | -2.6                |
| NSC23766         | 1    | 0.6                 |
|                  | 2    | -0.1                |
|                  | 3    | 0.2                 |
| Positive control | 1    | -1.2                |
|                  | 2    | 0.3                 |
|                  | 3    | -1.3                |
| Negative control | 1    | -0.9                |
|                  | 2    | -0.9                |



*6.d.iv. Murine skin biopsies from the different pre-treated groups showed neutrophil-rich infiltrate and dermal-epidermal separation as was observed in the positive control group.*

Skin biopsies of pre-treated mice showed dense infiltrates predominantly of neutrophils in the dermis, and dermal-epidermal separation. Serohemorrhagic crust formation was also observed in all different groups. Neutrophil-rich infiltrates were demonstrated in the group pre-treated with NSC23766, as well as in group pre-treated with dapsone (Figure 21). The same histological features were seen in the positive control group.

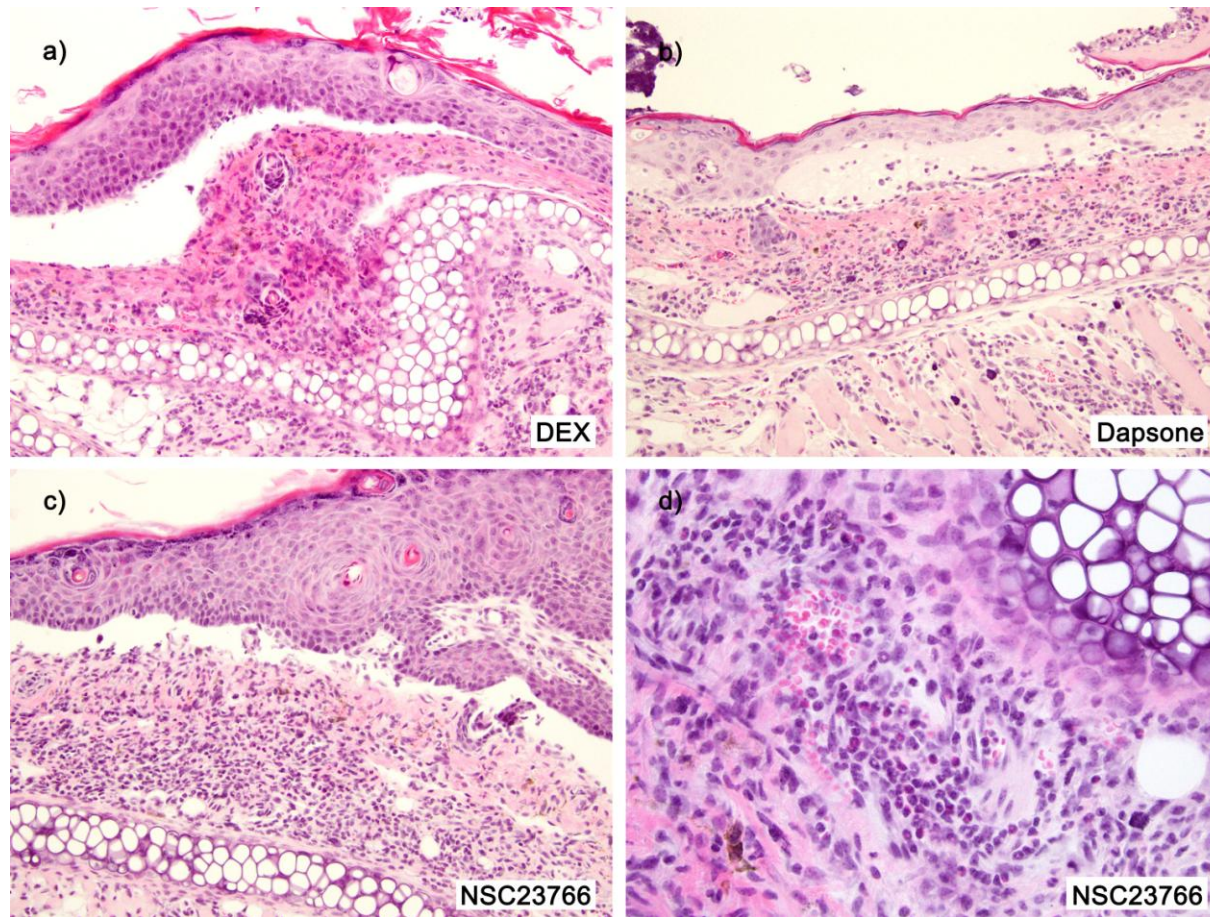


**Figure 21. Murine skin biopsies from each group of pre-treated mice, H&E.** a) Dermal-epidermal separation with moderate dermal infiltrate in a mouse pre-treated with dexamethasone (x20). b) Subepidermal bulla formation and dermal inflammatory infiltrate in a mouse pre-treated with dapsone. c) Dermal-epidermal separation with moderate dermal infiltrate in a mouse pre-treated with NSC23766. d) Infiltrate in a pre-treated mouse with NSC23766 showing the presence of neutrophils.



## **7. DISCUSSION**

---



## **7. DISCUSSION**

The passive transfer of 45 or 90 mg of rabbit anti-mCVIIICr IgG was capable of inducing the EBA phenotype in WT mice. Disease severity was demonstrated to be IgG dose-dependent, when evaluated by either both, BSA involvement or clinical score. Skin biopsies of lesional skin demonstrated the dermal granulocytic infiltrate associated with dermal-epidermal separation. Deposition of rabbit IgG and murine C3 was demonstrated in perilesional skin showing the activation of murine immune response to induce tissue damage. Clinical scores of our mice were similar to the ones obtained from the group of Sitaru et al. (43). However, weight loss and levels of specific anti-mCVIIICr antibodies were not statistically different when comparing both groups receiving different amount of antibodies. For the purpose of our project, and considering that both groups showed disease development, a 10 mg/day of rabbit anti-mCVIIICr IgG was considered enough to carry out further assays.

Based on the results obtained on the two sets of experiments performed in Rac2 KO mice, the deficiency of Rac2 protein has been shown to protect against EBA development after the passive transfer of rabbit anti-mCVIIICr IgG. Skin biopsies showed scattered infiltrate with no dermal-epidermal separation. With the deposition of rabbit IgG and mouse C3 at the BMZ (demonstrated both by DIF), a first step activation of murine immune response was demonstrated. Moreover the increased levels of circulating rabbit anti-mCVIIICr IgG throughout the observation time (by ELISA) showed the persistent impregnation of the mice with rabbit IgG. However, skin blistering, erosions, alopecia, serohemorrhagic crusts or weight loss did not develop in Rac2 KO mice. Surprisingly, studies of ALI induced in Rac2 KO mice showed the presence of neutrophils in the interstitium of the lung, yet not within alveolar spaces, which were mainly observed in sick WT mice (87). Compared to our results migration of neutrophils in the target tissue were not observed. The degree of inflammation in ALI studies were further assessed by: 1) the levels of chemokines and cytokines related with neutrophils recruitment, which were not significantly decreased

between WT and Rac2 KO mice; and 2) the levels of MPO were significantly decreased in Rac2 KO mice, which is what damage the lung tissue along with the secreted metalloproteinases. In our assays no experiments assessing chemokines and cytokines involved in neutrophil recruitment were performed, however no neutrophilic infiltrate was observed.

In contrast, the set of experiments performed with Rac2 inhibitor (NSC23766) did not affect or prevent the development of EBA after antibody exposure. Skin biopsies showed abundant neutrophilic infiltrate and dermal-epidermal separation, as was seen in the positive control group (non-pre-treated mice). However, there were many issues occurred while performing this set of experiment that will be further explained below. Yao et al. used the NSC23766 to prevent ALI induced on WT mice (88). Their results showed significant decrease in inflammatory cells infiltrate, such as neutrophils among others, as well as decrease in MPO activity ( $p=.01$  and  $p=.05$ , respectively). Greater inhibition of the inflammatory infiltrate was observed at higher doses (3mg/kg) of NSC23766 with similar results obtained in Dexamethasone group at 1 mg/Kg. Yet, marked decrease of neutrophils in the infiltrate was also observed at a lower dose (1 mg/kg) of NSC23766 (88). Regarding to our results, none of the pre-treated mice with NSC23766 had a significantly milder disease compared with the positive control group, and the skin biopsy showed moderate neutrophilic infiltrate similar to the positive control group.

Understanding the main pathways where Rac2 protein is involved, helps to elucidate and demonstrates the important role of neutrophils in EBA tissue injury, as well as the non-pathological effect of the isolated presence of antibodies and/or complement at the dermal-epidermal BMZ. Actually, recent research in EBA has been focused on neutrophils blockade, and its effect on chemotaxis and cellular function. This was also noted when reviewing each of the potential agents that are currently investigated for providing a benefit to EBA patients (mentioned in Table 4) (11).

As explained in the *Background* section, upon antibody-complement complex formation, neutrophils become crucial in tissue damage. This can be summarized in three steps: first, their recruitment to the skin; second, granulocyte activation; and third ROS formation and release. Some examples of molecules acting in the first step are GM-CSF as well as CXCL1/2 (orthologue of IL-8 in human). It has already been demonstrated that blockade of GM-CSF or CXCL1/2 or other molecules that induce the depletion of neutrophils such as neutrophil-depleting anti-Gr-1 antibody protects against disease development (74, 76, 94). The second step is started by the binding of the antibody-complement complex to the FcγRIV (orthologue of FcγRIIIA in human) of neutrophils, which induces activation of the immune response, and thus activation of neutrophils. Kasperkiewicz et al. could demonstrate that among all subtypes of FcγR, FcγRIV is exclusively required for EBA tissue injury, when compared with the other activating FcγR (79). Third, the ROS formation is induced by neutrophils by the limiting enzyme of NADPH oxidase. The best example for its requirement was the use of neutrophils from patients with CGD, as they lack NADPH oxidase. The *in vitro* incubation of those defective neutrophils with human skin and IgG against CVII failed to induce dermal-epidermal separation (76). Rac2 GTPase is involved in neutrophil recruitment and ROS release; therefore, by blocking Rac2 GTPase, previous step 1 and 3 are blocked as well. It is important to mention that EBA research experts are aware that there are still other non-well recognized cells intervening in tissue injury, however current assays show that the complete blockade of neutrophils are enough to avoid disease development, as our results confirmed (95).

Additionally, a current well-accepted EBA treatment is colchicine plus dapsone as first line therapy for mild and moderate disease (30, 96). Since colchicine inhibits the migration of neutrophils (by interfering with microtubules), and dapsone supposedly inhibits ROS formation (which mechanism is not yet clear), their combination might exert a similar effect as the one obtained from Rac2 deficiency or its blockade. This suggests the importance of this protein as a therapy target.



As shown herein, NSC23766 blocks Rac2 protein. However, this effect is not specific for Rac2, as it also inhibits Rac1, which is ubiquitously expressed and not limited to immune cells. Indeed, the main limitation of this study falls into the pharmacological inhibition of Rac2 protein, which could not demonstrate efficacy in neither avoiding nor inducing a milder EBA phenotype in mice. Several issues emerged while performing the set of experiments, including the administered drug dosage (a drug that has been used for many different conditions, including inflammation and cancer with distinct origins and behavior) and regimen of administration (ranging from single dosage for inflammatory conditions, to continuous administration with a pump (subcutaneous) for myeloproliferative disorders) (88, 91, 92). Furthermore, we suspect that NSC23766 has a narrow therapeutic window, as in our current study, intraperitoneal doses higher of 10 mg/d showed the sudden death in mice (this effect was not mentioned in the reviews published), and 7 mg/day could not show efficacy (87, 91, 92). Considering the natural course of EBA in this study's experimental animal model, it is possible that a continuous administration of NSC23766 (i.e. by subcutaneous implantation of a pump on mouse's back) may have produced improved outcomes. However, considering a drug with such a narrow therapeutic window along with the requirement of a pump in order to reach constant blood levels does not make this agent attractive for further investigation. While an increased interest in NSC23766 has been extremely related in its capability to inhibit Rac1 protein, no specific agents solely blocking Rac2 are currently available.

In regards to pre-treated mice with dapsons and dexamethasone, it is suspected that a longer pre-treatment period was likely required to prevent the development of EBA or to induce a milder EBA phenotype. Dose of dapsons used in our study was obtained from a study published regarding an experimental animal model of dermatitis herpetiformis. Two groups of mice were sensitized with gluten and treated afterwards. The first group was treated with gluten-free diet and dapsons, and the second group with gluten-free diet only. Resolution of blisters formation was observed after 1 week in the first group and after 2 – 3 weeks in the second group (93). It is difficult then to compare our results

with this study since our mice were initially healthy and no combined therapy was performed. Finally, because the inhibitor of the target protein was not successful; this part of the experiment was withdrawn after all the issues surfaced. Moreover, the benefit of dexamethasone and dapsona in humans has already been demonstrated in the literature.

From this point, further research in the development of more specific molecules that can effectively block Rac2 protein is required. For instance, 1) by developing new molecules with a higher affinity to GEFs that activate specifically Rac2, or 2) targeting the binding point between GTP and Rac2 (as occurs in the human Rac2 mutation, causing Rac2 deficiency), or 3) by directly competing with Rac2 protein when assembling to NADPH oxidase. The latter could be centered on the C-terminal sequence of Rac2 that differs from Rac1, and which has been exclusively related to the NADPH activation as demonstrated by the group of Yamauchi et al (84). Finding a specific blocker of this domain would increase specificity in inhibiting the Rac2 protein.

Additional research on Rac2 protein involvement in EBA pathogenesis would be by inducing the active animal model of EBA in Rac2 KO mice (by injecting mCVIICR protein instead of the specific IgG), since Rac2 protein is involved in T-cell development, and a CD4+ T-cell clone has been shown to participate in EBA development. It was mentioned already that exclusive Rac2 KO mice does not produce T-cell development abnormalities, however this has been studied in mice inducing immune response by bacteria products (such as fMLP a chemotactic peptide of neutrophils released by bacteria) instead of inducing immune response with self-proteins (loss of tolerance). A group studying the genetic diversity of *RAC2* gene has demonstrated susceptibility to certain autoimmune disease such as Multiple sclerosis ( $p=.022$ ) and Chron's Disease ( $p=048$ ), yet, the authors affirmed that these results required of further validation (97). Other observations from this experimental active animal model could also answer whether Rac2 protein has an

additional inhibitory effect in neutrophils similar to GM-CSF, which has shown to affect antibody production by blocking the B-cell helper neutrophils (74).

The main limitation of this research project is whether these data obtained from mice can be extrapolated to human EBA. A starting point to answer this question could be performing *in vitro* experiments by cryosection models, incubating patient's anti-CVII IgG with normal skin and further adding neutrophils lacking Rac2 protein. This experiment would focus only on the ROS formation induced by NADPH oxidase (since migration of neutrophils would be the step already passed over). Due to the deficiency of Rac2 protein, ROS would not be released; and dermal-epidermal separation would be prevented.

To finalize, the pathophysiology of EBA remains only partially understood and requires further studies to clarify ambiguities. Research is centered to investigate target therapies that involve different areas of EBA pathogenesis, going from the initial loss of immune tolerance to the last effector phase of tissue damaging. With the current animal models available, chances to research new target molecules are high. Moreover, due to the rarity of the disease in the population, we foresee difficulties in testing new developed molecules in the human context.

## **8. CONCLUSIONS**

---



## **8. CONCLUSIONS**

EBA is a rare and refractory autoimmune skin disease that requires attention in specialized health centers in order to achieve a correct and fast diagnosis and a proper treatment. The chronicity of this disease, as well as its refractoriness to most of the today's available treatments, makes EBA patients' management extremely challenging. All current therapies are not specific and associated with multiple short and long-term side effects.

Innate immunity is strongly involved in EBA, with the activation of neutrophils and ROS formation being essential events in the development of clinical manifestations of EBA. In the present study we demonstrate that the Rac2 protein, which is involved in both neutrophil chemotaxis and activation (including ROS synthesis by activation of NADPH oxidase and release of proteolytic enzymes), is crucial in the pathogenesis of experimental EBA in animal models. This protein represents a new therapeutic target (Rac2) for developing new systems to treat patients with EBA and other IgG-mediated organ-specific autoimmune diseases, where neutrophils play a central role.

We have been unable to demonstrate the efficacy of the pharmacological inhibition of Rac2 protein (NSC23766) in passively induced EBA in wild-type mice. Possible underlying mechanisms that may explain this lack of efficacy are discussed. Further efforts are required to develop effective, more selective and non-toxic drugs for these patients.



## **9. REFERENCES**

---





## 9. REFERENCES

1. Hashmi S, Marinkovich MP. Molecular organization of the basement membrane zone. *Clin Dermatol*. 2011;29(4):398-411.
2. Turcan I, Jonkman MF. Blistering disease: insight from the hemidesmosome and other components of the dermal-epidermal junction. *Cell Tissue Res*. 2015;360(3):545-69.
3. Baum S, Sakka N, Artsi O, Trau H, Barzilai A. Diagnosis and classification of autoimmune blistering diseases. *Autoimmun Rev*. 2014;13(4-5):482-9.
4. Dainichi T, Koga H, Tsuji T, Ishii N, Ohyama B, Ueda A, et al. From anti-p200 pemphigoid to anti-laminin gamma1 pemphigoid. *J Dermatol*. 2010;37(3):231-8.
5. Yayli S, Pelivani N, Beltraminelli H, Wirthmuller U, Beleznay Z, Horn M, et al. Detection of linear IgE deposits in bullous pemphigoid and mucous membrane pemphigoid: a useful clue for diagnosis. *Br J Dermatol*. 2011;165(5):1133-7.
6. Hashimoto T, Ishii N, Ohata C, Furumura M. Pathogenesis of epidermolysis bullosa acquisita, an autoimmune subepidermal bullous disease. *J Pathol*. 2012;228(1):1-7.
7. Elliot G. Two cases of epidermolysis bullosa. *Journal of Cutaneous Genitourinary Disease*. 1895;13:10.
8. R. K. Ein Beitrag zur Frage der Epidermolysis Bullosa (Hereditary et Aquisita). *These Inaug Rostock Diss*. 1904.
9. Kim JH, Kim SC. Epidermolysis bullosa acquisita. *J Eur Acad Dermatol Venereol*. 2013;27(10):1204-13.
10. Zhu XJ, Niimi Y, Bystryk JC. Epidermolysis bullosa acquisita. Incidence in patients with basement membrane zone antibodies. *Arch Dermatol*. 1990;126(2):171-4.
11. Ludwig RJ. Clinical presentation, pathogenesis, diagnosis, and treatment of epidermolysis bullosa acquisita. *ISRN Dermatol*. 2013;2013:812029.
12. Gupta R, Woodley DT, Chen M. Epidermolysis bullosa acquisita. *Clin Dermatol*. 2012;30(1):60-9.

13. Lee CW. Prevalences of subacute cutaneous lupus erythematosus and Epidermolysis bullosa acquisita among Korean/Oriental populations. *Dermatology*. 1998;197(2):187.
14. Zumelzu C, Le Roux-Villet C, Loiseau P, Busson M, Heller M, Aucouturier F, et al. Black patients of African descent and HLA-DRB1\*15:03 frequency overrepresented in epidermolysis bullosa acquisita. *J Invest Dermatol*. 2011;131(12):2386-93.
15. Lee CW, Kim SC, Han H. Distribution of HLA class II alleles in Korean patients with epidermolysis bullosa acquisita. *Dermatology*. 1996;193(4):328-9.
16. Callot-Mellot C, Bodemer C, Caux F, Bourgault-Villada I, Fraitag S, Goudie G, et al. Epidermolysis bullosa acquisita in childhood. *Arch Dermatol*. 1997;133(9):1122-6.
17. Mayuzumi M, Akiyama M, Nishie W, Ukae S, Abe M, Sawamura D, et al. Childhood epidermolysis bullosa acquisita with autoantibodies against the noncollagenous 1 and 2 domains of type VII collagen: case report and review of the literature. *Br J Dermatol*. 2006;155(5):1048-52.
18. Abrams ML, Smidt A, Benjamin L, Chen M, Woodley D, Mancini AJ. Congenital epidermolysis bullosa acquisita: vertical transfer of maternal autoantibody from mother to infant. *Arch Dermatol*. 2011;147(3):337-41.
19. Kim JH, Kim YH, Kim S, Noh EB, Kim SE, Vorobyev A, et al. Serum levels of anti-type VII collagen antibodies detected by enzyme-linked immunosorbent assay in patients with epidermolysis bullosa acquisita are correlated with the severity of skin lesions. *J Eur Acad Dermatol Venereol*. 2013;27(2):e224-30.
20. Marzano AV, Cozzani E, Fanoni D, De Pita O, Vassallo C, Berti E, et al. Diagnosis and disease severity assessment of epidermolysis bullosa acquisita by ELISA for anti-type VII collagen autoantibodies: an Italian multicentre study. *Br J Dermatol*. 2013;168(1):80-4.
21. Ishii N, Recke A, Mihai S, Hirose M, Hashimoto T, Zillikens D, et al. Autoantibody-induced intestinal inflammation and weight loss in experimental epidermolysis bullosa acquisita. *J Pathol*. 2011;224(2):234-44.

22. Terra JB, Meijer JM, Jonkman MF, Diercks GF. The n- vs. u-serration is a learnable criterion to differentiate pemphigoid from epidermolysis bullosa acquisita in direct immunofluorescence serration pattern analysis. *Br J Dermatol.* 2013;169(1):100-5.
23. Vodegel RM, Jonkman MF, Pas HH, de Jong MC. U-serrated immunodeposition pattern differentiates type VII collagen targeting bullous diseases from other subepidermal bullous autoimmune diseases. *Br J Dermatol.* 2004;151(1):112-8.
24. Komorowski L, Muller R, Vorobyev A, Probst C, Recke A, Jonkman MF, et al. Sensitive and specific assays for routine serological diagnosis of epidermolysis bullosa acquisita. *J Am Acad Dermatol.* 2013;68(3):e89-95.
25. Saleh MA, Ishii K, Kim YJ, Murakami A, Ishii N, Hashimoto T, et al. Development of NC1 and NC2 domains of type VII collagen ELISA for the diagnosis and analysis of the time course of epidermolysis bullosa acquisita patients. *J Dermatol Sci.* 2011;62(3):169-75.
26. De Jong MC, Bruins S, Heeres K, Jonkman MF, Nieboer C, Boorsma DM, et al. Bullous pemphigoid and epidermolysis bullosa acquisita. Differentiation by fluorescence overlay antigen mapping. *Arch Dermatol.* 1996;132(2):151-7.
27. Kazama T, Yamamoto Y, Hashimoto T, Komai A, Ito M. Application of confocal laser scanning microscopy to differential diagnosis of bullous pemphigoid and epidermolysis bullosa acquisita. *Br J Dermatol.* 1998;138(4):593-601.
28. Yaoita H, Briggaman RA, Lawley TJ, Provost TT, Katz SI. Epidermolysis bullosa acquisita: ultrastructural and immunological studies. *J Invest Dermatol.* 1981;76(4):288-92.
29. Bozeman PM, Learn DB, Thomas EL. Inhibition of the human leukocyte enzymes myeloperoxidase and eosinophil peroxidase by dapsone. *Biochem Pharmacol.* 1992;44(3):553-63.
30. Intong LR, Murrell DF. Management of epidermolysis bullosa acquisita. *Dermatol Clin.* 2011;29(4):643-7.
31. Gurcan HM, Ahmed AR. Current concepts in the treatment of epidermolysis bullosa acquisita. *Expert Opin Pharmacother.* 2011;12(8):1259-68.

32. Arora KP, Sachdeva B, Singh N, Bhattacharya SN. Remission of recalcitrant epidermolysis bullosa acquisita (EBA) with colchicine monotherapy. *J Dermatol.* 2005;32(2):114-9.
33. Maize JC, Jr., Cohen JB. Cyclosporine controls epidermolysis bullosa acquisita co-occurring with acquired factor VIII deficiency. *Int J Dermatol.* 2005;44(8):692-4.
34. Kowalick L, Suckow S, Ziegler H, Waldmann T, Ponnighaus JM, Glaser V. Mycophenolate mofetil in epidermolysis bullosa acquisita. *Dermatology.* 2003;207(3):332-4.
35. Tran MM, Anhalt GJ, Barrett T, Cohen BA. Childhood IgA-mediated epidermolysis bullosa acquisita responding to mycophenolate mofetil as a corticosteroid-sparing agent. *J Am Acad Dermatol.* 2006;54(4):734-6.
36. Kasperkiewicz M, Muller R, Manz R, Magens M, Hammers CM, Somlai C, et al. Heat-shock protein 90 inhibition in autoimmunity to type VII collagen: evidence that nonmalignant plasma cells are not therapeutic targets. *Blood.* 2011;117(23):6135-42.
37. Alban S, Ludwig RJ, Bendas G, Schon MP, Oostingh GJ, Radeke HH, et al. PS3, a semisynthetic beta-1,3-glucan sulfate, diminishes contact hypersensitivity responses through inhibition of L- and P-selectin functions. *J Invest Dermatol.* 2009;129(5):1192-202.
38. Citro A, Cantarelli E, Maffi P, Nano R, Melzi R, Mercalli A, et al. CXCR1/2 inhibition enhances pancreatic islet survival after transplantation. *J Clin Invest.* 2012;122(10):3647-51.
39. Magnusson SE, Andren M, Nilsson KE, Sondermann P, Jacob U, Kleinau S. Amelioration of collagen-induced arthritis by human recombinant soluble Fc $\gamma$ RIIb. *Clin Immunol.* 2008;127(2):225-33.
40. Chen Q, He F, Kwang J, Chan JK, Chen J. GM-CSF and IL-4 stimulate antibody responses in humanized mice by promoting T, B, and dendritic cell maturation. *J Immunol.* 2012;189(11):5223-9.

41. Ishii N, Hamada T, Dainichi T, Karashima T, Nakama T, Yasumoto S, et al. Epidermolysis bullosa acquisita: what's new? *J Dermatol.* 2010;37(3):220-30.
42. Sitaru C. Experimental models of epidermolysis bullosa acquisita. *Exp Dermatol.* 2007;16(6):520-31.
43. Sitaru C, Mihai S, Otto C, Chiriac MT, Hausser I, Dotterweich B, et al. Induction of dermal-epidermal separation in mice by passive transfer of antibodies specific to type VII collagen. *J Clin Invest.* 2005;115(4):870-8.
44. Woodley DT, Chang C, Saadat P, Ram R, Liu Z, Chen M. Evidence that anti-type VII collagen antibodies are pathogenic and responsible for the clinical, histological, and immunological features of epidermolysis bullosa acquisita. *J Invest Dermatol.* 2005;124(5):958-64.
45. Woodley DT, Ram R, Doostan A, Bandyopadhyay P, Huang Y, Remington J, et al. Induction of epidermolysis bullosa acquisita in mice by passive transfer of autoantibodies from patients. *J Invest Dermatol.* 2006;126(6):1323-30.
46. Sitaru C, Chiriac MT, Mihai S, Buning J, Gebert A, Ishiko A, et al. Induction of complement-fixing autoantibodies against type VII collagen results in subepidermal blistering in mice. *J Immunol.* 2006;177(5):3461-8.
47. Sitaru C, Kromminga A, Hashimoto T, Brocker EB, Zillikens D. Autoantibodies to type VII collagen mediate Fc $\gamma$ -dependent neutrophil activation and induce dermal-epidermal separation in cryosections of human skin. *Am J Pathol.* 2002;161(1):301-11.
48. Gammon WR, Inman AO, 3rd, Wheeler CE, Jr. Differences in complement-dependent chemotactic activity generated by bullous pemphigoid and epidermolysis bullosa acquisita immune complexes: demonstration by leukocytic attachment and organ culture methods. *J Invest Dermatol.* 1984;83(1):57-61.
49. Gammon WR, Heise ER, Burke WA, Fine JD, Woodley DT, Briggaman RA. Increased frequency of HLA-DR2 in patients with autoantibodies to epidermolysis bullosa acquisita antigen: evidence that the expression of autoimmunity to type VII collagen is HLA class II allele associated. *J Invest Dermatol.* 1988;91(3):228-32.

50. Woodley DT, Briggaman RA, O'Keefe EJ, Inman AO, Queen LL, Gammon WR. Identification of the skin basement-membrane autoantigen in epidermolysis bullosa acquisita. *N Engl J Med*. 1984;310(16):1007-13.
51. Ludwig RJ, Zillikens D. Pathogenesis of epidermolysis bullosa acquisita. *Dermatol Clin*. 2011;29(3):493-501, xi.
52. Sesarman A, Sitaru AG, Olaru F, Zillikens D, Sitaru C. Neonatal Fc receptor deficiency protects from tissue injury in experimental epidermolysis bullosa acquisita. *J Mol Med (Berl)*. 2008;86(8):951-9.
53. Christiano AM, Rosenbaum LM, Chung-Honet LC, Parente MG, Woodley DT, Pan TC, et al. The large non-collagenous domain (NC-1) of type VII collagen is amino-terminal and chimeric. Homology to cartilage matrix protein, the type III domains of fibronectin and the A domains of von Willebrand factor. *Hum Mol Genet*. 1992;1(7):475-81.
54. Gammon WR, Abernethy ML, Padilla KM, Prisayanh PS, Cook ME, Wright J, et al. Noncollagenous (NC1) domain of collagen VII resembles multidomain adhesion proteins involved in tissue-specific organization of extracellular matrix. *J Invest Dermatol*. 1992;99(6):691-6.
55. Villone D, Fritsch A, Koch M, Bruckner-Tuderman L, Hansen U, Bruckner P. Supramolecular interactions in the dermo-epidermal junction zone: anchoring fibril-collagen VII tightly binds to banded collagen fibrils. *J Biol Chem*. 2008;283(36):24506-13.
56. Chen M, Marinkovich MP, Veis A, Cai X, Rao CN, O'Toole EA, et al. Interactions of the amino-terminal noncollagenous (NC1) domain of type VII collagen with extracellular matrix components. A potential role in epidermal-dermal adherence in human skin. *J Biol Chem*. 1997;272(23):14516-22.
57. Chen M, Marinkovich MP, Jones JC, O'Toole EA, Li YY, Woodley DT. NC1 domain of type VII collagen binds to the beta3 chain of laminin 5 via a unique subdomain within the fibronectin-like repeats. *J Invest Dermatol*. 1999;112(2):177-83.

58. Woodley DT, Burgeson RE, Lunstrum G, Bruckner-Tuderman L, Reese MJ, Briggaman RA. Epidermolysis bullosa acquisita antigen is the globular carboxyl terminus of type VII procollagen. *J Clin Invest.* 1988;81(3):683-7.
59. Lapiere JC, Woodley DT, Parente MG, Iwasaki T, Wynn KC, Christiano AM, et al. Epitope mapping of type VII collagen. Identification of discrete peptide sequences recognized by sera from patients with acquired epidermolysis bullosa. *J Clin Invest.* 1993;92(4):1831-9.
60. Gammon WR, Murrell DF, Jenison MW, Padilla KM, Prisayanh PS, Jones DA, et al. Autoantibodies to type VII collagen recognize epitopes in a fibronectin-like region of the noncollagenous (NC1) domain. *J Invest Dermatol.* 1993;100(5):618-22.
61. Chen M, Doostan A, Bandyopadhyay P, Remington J, Wang X, Hou Y, et al. The cartilage matrix protein subdomain of type VII collagen is pathogenic for epidermolysis bullosa acquisita. *Am J Pathol.* 2007;170(6):2009-18.
62. Ishii N, Yoshida M, Hisamatsu Y, Ishida-Yamamoto A, Nakane H, Iizuka H, et al. Epidermolysis bullosa acquisita sera react with distinct epitopes on the NC1 and NC2 domains of type VII collagen: study using immunoblotting of domain-specific recombinant proteins and postembedding immunoelectron microscopy. *Br J Dermatol.* 2004;150(5):843-51.
63. Ishii N, Yoshida M, Ishida-Yamamoto A, Fritsch A, Elfert S, Bruckner-Tuderman L, et al. Some epidermolysis bullosa acquisita sera react with epitopes within the triple-helical collagenous domain as indicated by immunoelectron microscopy. *Br J Dermatol.* 2009;160(5):1090-3.
64. Chen M, Keene DR, Costa FK, Tahk SH, Woodley DT. The carboxyl terminus of type VII collagen mediates antiparallel dimer formation and constitutes a new antigenic epitope for epidermolysis Bullosa acquisita autoantibodies. *J Biol Chem.* 2001;276(24):21649-55.
65. Vorobyev A, Ujiie H, Recke A, Buijsrogge JJ, Jonkman MF, Pas HH, et al. Autoantibodies to Multiple Epitopes on the Non-Collagenous-1 Domain of Type VII Collagen Induce Blisters. *J Invest Dermatol.* 2015;135(6):1565-73.



66. Csorba K, Chiriac MT, Florea F, Ghinia MG, Licarete E, Rados A, et al. Blister-inducing antibodies target multiple epitopes on collagen VII in mice. *J Cell Mol Med.* 2014;18(9):1727-39.
67. Sitaru AG, Sesarman A, Mihai S, Chiriac MT, Zillikens D, Hultman P, et al. T cells are required for the production of blister-inducing autoantibodies in experimental epidermolysis bullosa acquisita. *J Immunol.* 2010;184(3):1596-603.
68. Muller R, Dahler C, Mobs C, Wenzel E, Eming R, Messer G, et al. T and B cells target identical regions of the non-collagenous domain 1 of type VII collagen in epidermolysis bullosa acquisita. *Clin Immunol.* 2010;135(1):99-107.
69. Tukaj S, Hellberg L, Ueck C, Hansel M, Samavedam U, Zillikens D, et al. Heat shock protein 90 is required for ex vivo neutrophil-driven autoantibody-induced tissue damage in experimental epidermolysis bullosa acquisita. *Exp Dermatol.* 2015;24(6):471-3.
70. Tukaj S, Zillikens D, Kasperkiewicz M. Heat shock protein 90: a pathophysiological factor and novel treatment target in autoimmune bullous skin diseases. *Exp Dermatol.* 2015;24(8):567-71.
71. Woodley DT, Remington J, Chen M. Autoimmunity to type VII collagen: epidermolysis bullosa acquisita. *Clin Rev Allergy Immunol.* 2007;33(1-2):78-84.
72. Sesarman A, Mihai S, Chiriac MT, Olaru F, Sitaru AG, Thurman JM, et al. Binding of avian IgY to type VII collagen does not activate complement and leucocytes and fails to induce subepidermal blistering in mice. *Br J Dermatol.* 2008;158(3):463-71.
73. Mihai S, Chiriac MT, Takahashi K, Thurman JM, Holers VM, Zillikens D, et al. The alternative pathway of complement activation is critical for blister induction in experimental epidermolysis bullosa acquisita. *J Immunol.* 2007;178(10):6514-21.
74. Samavedam UK, Iwata H, Muller S, Schulze FS, Recke A, Schmidt E, et al. GM-CSF modulates autoantibody production and skin blistering in experimental epidermolysis bullosa acquisita. *J Immunol.* 2014;192(2):559-71.
75. Simon D, Borradori L, Simon HU. Glucocorticoids in autoimmune bullous diseases: are neutrophils the key cellular target? *J Invest Dermatol.* 2013;133(10):2314-5.

76. Chiriac MT, Roesler J, Sindrilaru A, Scharffetter-Kochanek K, Zillikens D, Sitaru C. NADPH oxidase is required for neutrophil-dependent autoantibody-induced tissue damage. *J Pathol.* 2007;212(1):56-65.
77. Nimmerjahn F, Ravetch JV. Antibody-mediated modulation of immune responses. *Immunol Rev.* 2010;236:265-75.
78. Ambrosius H, Hadge D. Chicken immunoglobulins. *Vet Immunol Immunopathol.* 1987;17(1-4):57-67.
79. Kasperkiewicz M, Nimmerjahn F, Wende S, Hirose M, Iwata H, Jonkman MF, et al. Genetic identification and functional validation of FcγR4 as key molecule in autoantibody-induced tissue injury. *J Pathol.* 2012;228(1):8-19.
80. Filip-Ciubotaru F, Manciu C, Stoleriu G, Foia L. NADPH Oxidase: Structure and Activation Mechanisms (Review). Note I. *Rev Med Chir Soc Med Nat Iasi.* 2016;120(1):29-33.
81. Bedard K, Krause KH. The NOX family of ROS-generating NADPH oxidases: physiology and pathophysiology. *Physiol Rev.* 2007;87(1):245-313.
82. Pai SY, Kim C, Williams DA. Rac GTPases in human diseases. *Dis Markers.* 2010;29(3-4):177-87.
83. Gu Y, Williams DA. RAC2 GTPase deficiency and myeloid cell dysfunction in human and mouse. *J Pediatr Hematol Oncol.* 2002;24(9):791-4.
84. Zhang H, Sun C, Glogauer M, Bokoch GM. Human neutrophils coordinate chemotaxis by differential activation of Rac1 and Rac2. *J Immunol.* 2009;183(4):2718-28.
85. Pick E. Role of the Rho GTPase Rac in the activation of the phagocyte NADPH oxidase: outsourcing a key task. *Small GTPases.* 2014;5:e27952.
86. Yamauchi A, Marchal CC, Molitoris J, Pech N, Knaus U, Towe J, et al. Rac GTPase isoform-specific regulation of NADPH oxidase and chemotaxis in murine neutrophils in vivo. Role of the C-terminal polybasic domain. *J Biol Chem.* 2005;280(2):953-64.

87. Dooley JL, Abdel-Latif D, St Laurent CD, Puttagunta L, Befus D, Lacy P. Regulation of inflammation by Rac2 in immune complex-mediated acute lung injury. *Am J Physiol Lung Cell Mol Physiol*. 2009;297(6):L1091-102.
88. Yao HY, Chen L, Xu C, Wang J, Chen J, Xie QM, et al. Inhibition of Rac activity alleviates lipopolysaccharide-induced acute pulmonary injury in mice. *Biochim Biophys Acta*. 2011;1810(7):666-74.
89. Csorba K, Sesarman A, Oswald E, Feldrihan V, Fritsch A, Hashimoto T, et al. Cross-reactivity of autoantibodies from patients with epidermolysis bullosa acquisita with murine collagen VII. *Cell Mol Life Sci*. 2010;67(8):1343-51.
90. Olaru F, Mihai S, Petrescu I, Zillikens D, Sitaru C. Generation and characterization of monoclonal antibodies against the intracellular domain of hemidesmosomal type XVII collagen. *Hybridoma (Larchmt)*. 2006;25(3):158-62.
91. Binker MG, Binker-Cosen AA, Gaisano HY, Cosen-Binker LI. Inhibition of Rac1 decreases the severity of pancreatitis and pancreatitis-associated lung injury in mice. *Exp Physiol*. 2008;93(10):1091-103.
92. Thomas EK, Cancelas JA, Chae HD, Cox AD, Keller PJ, Perrotti D, et al. Rac guanosine triphosphatases represent integrating molecular therapeutic targets for BCR-ABL-induced myeloproliferative disease. *Cancer Cell*. 2007;12(5):467-78.
93. Marietta E, Black K, Camilleri M, Krause P, Rogers RS, 3rd, David C, et al. A new model for dermatitis herpetiformis that uses HLA-DQ8 transgenic NOD mice. *J Clin Invest*. 2004;114(8):1090-7.
94. Sadeghi H, Lockmann A, Hund AC, Samavedam UK, Papi E, Vafia K, et al. Caspase-1-independent IL-1 release mediates blister formation in autoantibody-induced tissue injury through modulation of endothelial adhesion molecules. *J Immunol*. 2015;194(8):3656-63.
95. Kasperkiewicz M, Sadik CD, Bieber K, Ibrahim SM, Manz RA, Schmidt E, et al. Epidermolysis Bullosa Acquisita: From Pathophysiology to Novel Therapeutic Options. *J Invest Dermatol*. 2016;136(1):24-33.

96. Hughes AP, Callen JP. Epidermolysis bullosa acquisita responsive to dapsone therapy. *J Cutan Med Surg.* 2001;5(5):397-9.
97. Sironi M, Guerini FR, Agliardi C, Biasin M, Cagliani R, Fumagalli M, et al. An evolutionary analysis of RAC2 identifies haplotypes associated with human autoimmune diseases. *Mol Biol Evol.* 2011;28(12):3319-29.